Winkler *Swiss Journal of Geosciences* (2024) 117:4
https://doi.org/10.1186/s00015-024-00454-7

SGG SGS sc | nat
Swiss Journal of Geosciences

ORIGINAL PAPER Open Access

The North Penninic Bündnerschiefer and Flysch of the Prättigau (Swiss Alps) revisited

Wilfried Winkler[1*]

Abstract

During the re-mapping of the area for the Geological Atlas of Switzerland, a significant stratigraphic unconformity was discovered in the North Penninic (Valais) Bündnerschiefer and the Flysch series of the northern Prättigau. It separates different units of the Cretaceous Bündnerschiefer from the Palaeogene Flysch. We explain this observation by a basin conversion from extension to compression, which caused the initial deformation of the Bündnerschiefer in an accretionary wedge. Interlinked return-flow has created a new heterogeneous substrate for the flysch sediments and explains the different types of unconformities. The basin conversion coincided with high-grade metamorphism in the vicinity of the the South Penninic suture and the Austroalpine units, and the increased exhumation in the Austroalpine nappe stack. Detrital zircon dating confirms also a change from European to Austroalpine detrital sources in the flysch sandstones. We discuss a palaeotectonic model leading to hP/IT metamorphism of the Bündnerschiefer in the Late Eocene (c. 42 Ma). It appears that the flysch formations were also involved, but to a lesser degree by tectonic deformation from the late Early Eocene onwards, as the pervasive folding characteristic of the Bündnerschiefer is absent. This has been followed by a phase of S-directed backfolding. During the Oligocene and Miocene, more extensive deformation occurred by SE to NW compression and finally by probable westward thrusting and folding. Our main theme is the transition from passive to active continental margins, which in Alpine plate tectonic framework corresponds to the transition to flysch sedimentation by basin conversion. Our results show that the simultaneity of the transition from extension to compression, as indicated by the accumulation of flysch, shifted in time from south to north in the Alpine Tethys.

Keywords Prättigau half-window, Cretaceous-Palaeogene, Stratigraphy, Palaeogeography, Basin conversion, Tectonics

1 Introduction and geological framework

The Alpine Tethys formed between the Eurasian and African continental plates from the Triassic to the end of the Eocene (Fig. 1). It is thought to have been opened by two major opposing shear zones (Steinmann, 1994, Ribes et al., 2019) in which asthenospheric mantle was exhumed, first in the South Penninic and then in the North Penninic domains. In the Triassic series, extensional volcanism is manifested in the Apulian (African) margin in the Austroalpine and South Alpine palaeogeographic realms (e.g. Furrer et al., 2008, Beltràn et al., 2016). Basin conversion and subduction, accompanied by flysch deposition, began first in the South Penninic in the Late Cretaceous and, according to current knowledge, in the North Penninic basins at the Cretaceous-Tertiary boundary. By the end of the Miocene, the collision between Africa (the Adriatic Indenter) and Europe had been completed. Foreland basins formed on both sides of the Alps, which also received syn-sedimentary volcanic debris from late Alpine volcanism (e.g., Lu et al., 2019). The Early Cretaceous to Early Eocene sedimentary units

Editorial handling: Adrian Pfiffner

*Correspondence:
Wilfried Winkler
wilfried.winkler@erdw.ethz.ch
[1] Geological Institute, Department of Earth Sciences, ETH Zurich, Sonneggstrasse 5, 8092 Zurich, Switzerland

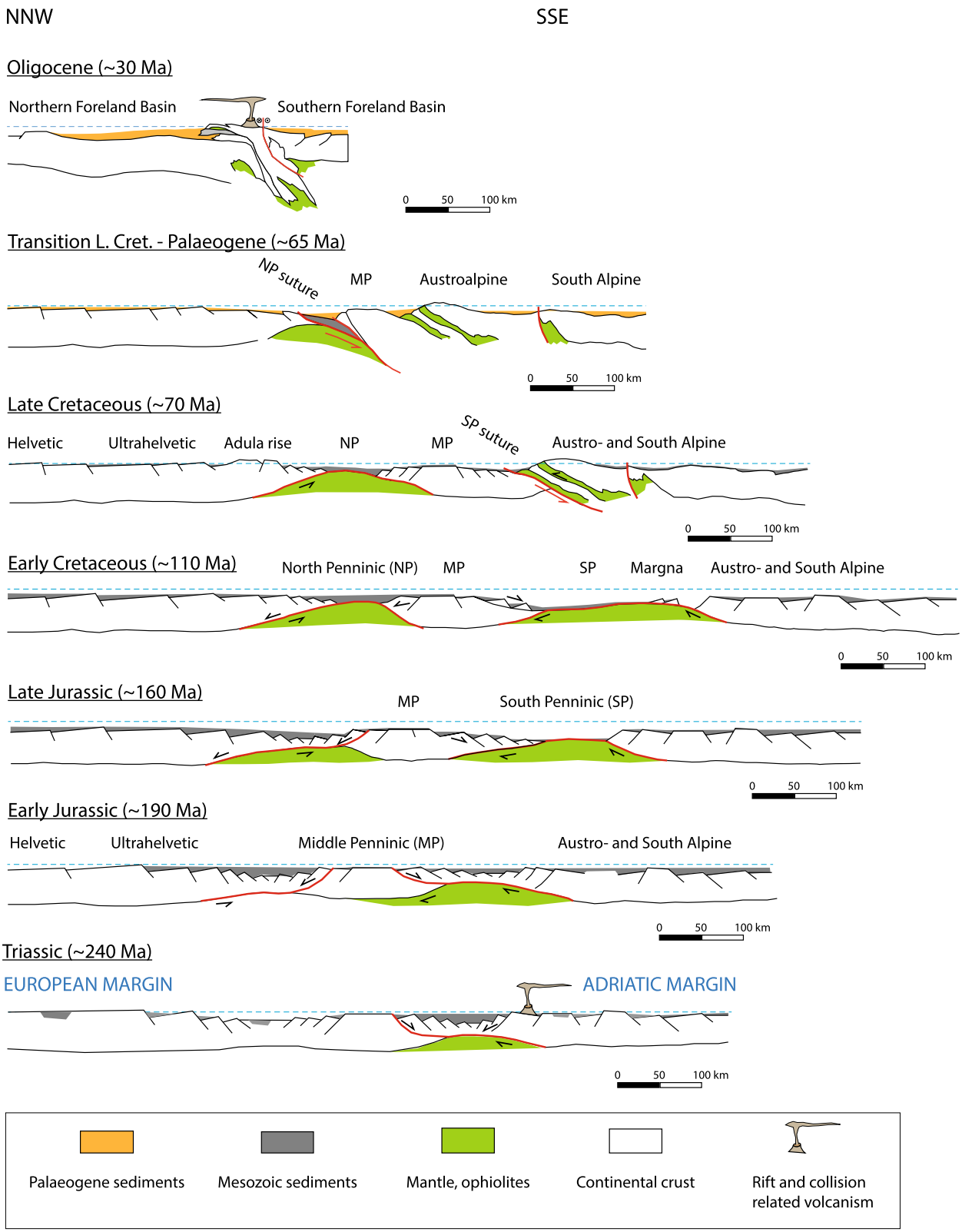

Fig. 1 Schematic representation of palaeogeographic profiles in time across the Alpine Tethys. Inspired by Trümpy (1980), Matter et al. (1980), Steinmann (1994), Handy et al. (2010), Ribes et al. (2019) and others

of the North Penninic palaeogeographical realm (Fig. 1) are the subject of this paper. We refer to the Cretaceous sedimentary series by the internationally known name Bündnerschiefer ("Grisons schists"). The sediments associated with the subsequent subduction are known as Flysch.

In the eastern Swiss Alps, the exhumation and erosion of higher nappes offers a close insight into the North Penninic Bündnerschiefer and Flysch units of the Prättigau (Fig. 2, 3). The Prättigau half-window (e.g., Steinmann, 1994, Weh and Froitzheim, 2001, Schmid et al., 2004) comprises sedimentary units which witness the Early Cretaceous to Early Eocene depositional history in the external North Penninic palaeogeographic realm. The Prättigau sedimentary sequence is internally deformed. It overthrusts Helvetic nappes at its base and is itself overthrusted by the Middle Penninic and Austroalpine basement and sedimentary units. In the Tomül nappe relics of oceanic basement rocks with a depleted mantle source are reported (Steinmann, 1994, Steinmann and Stille, 1999). In general, however, only a few occurrences of oceanic basement rocks are known in the North Penninic and Valaisan basin units of the Western Alps (e.g. Schmid et al., 2004).

The frame of the half-window is formed by the tectonically superimposed sedimentary Middle Penninic Falknis and Sulzfluh nappes (Fig. 3b), and by Austroalpine basement and sedimentary cover nappes (Silvretta and Oetztal Crystalline nappes, respectively, and the Upper Austroalpine cover nappes called Northern Calcareous

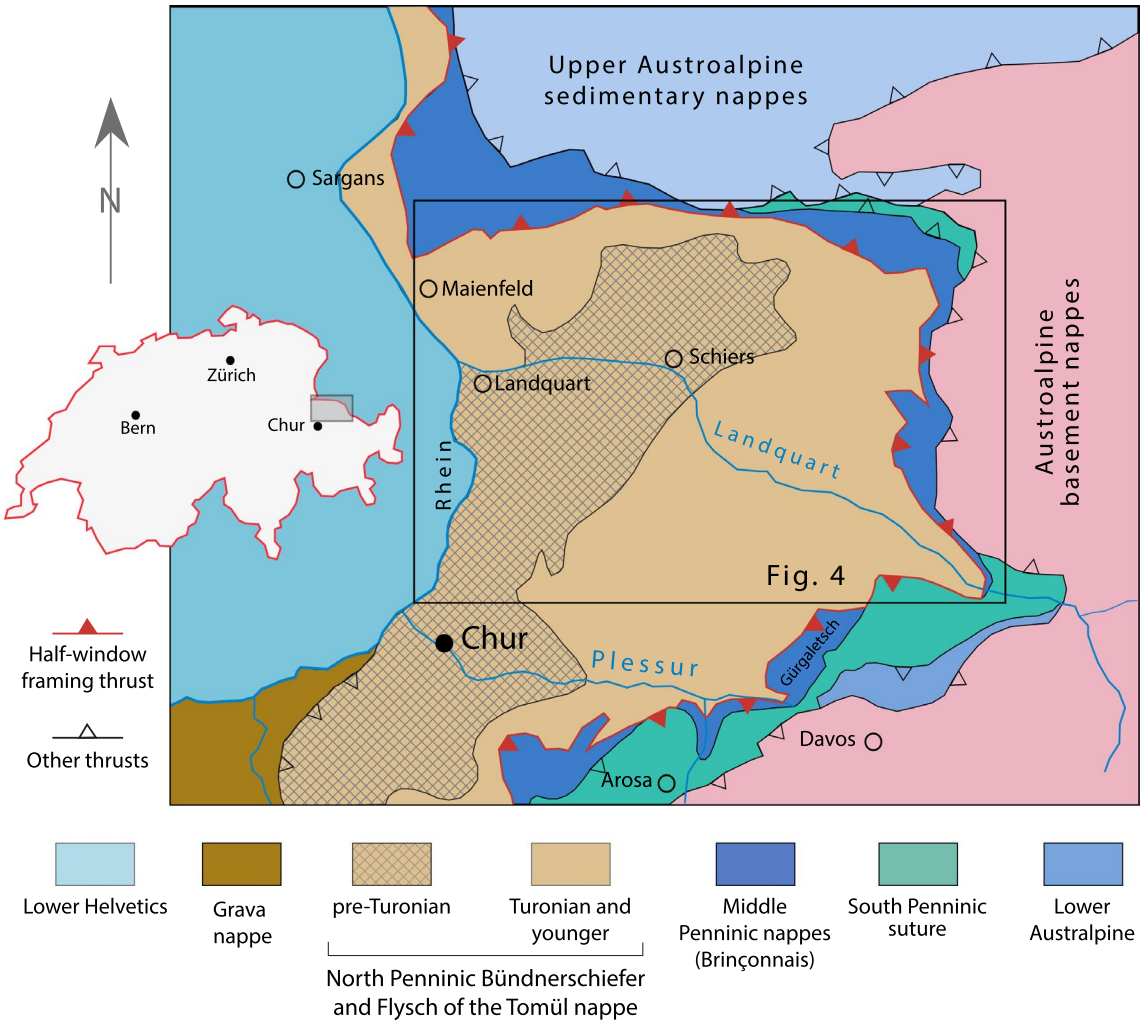

Fig. 2 Overview map of the tectonic units forming the Prättigau half-window. The rectangle shows the map in Fig. 4. The conservative representation of the units in the Prättigau half-window distinguishes between pre-Turonian Bündnerschiefer and post-Turonian Flysch formations as drawn e.g., by Nänny (1948), Steinmann (1994), Weh and Froitzheim (2001), Schmid et al. (2004), Bundesamt für Landestopografie swisstopo (2005). Note that the regional distribution of flysch formations will be strongly modified by the present study

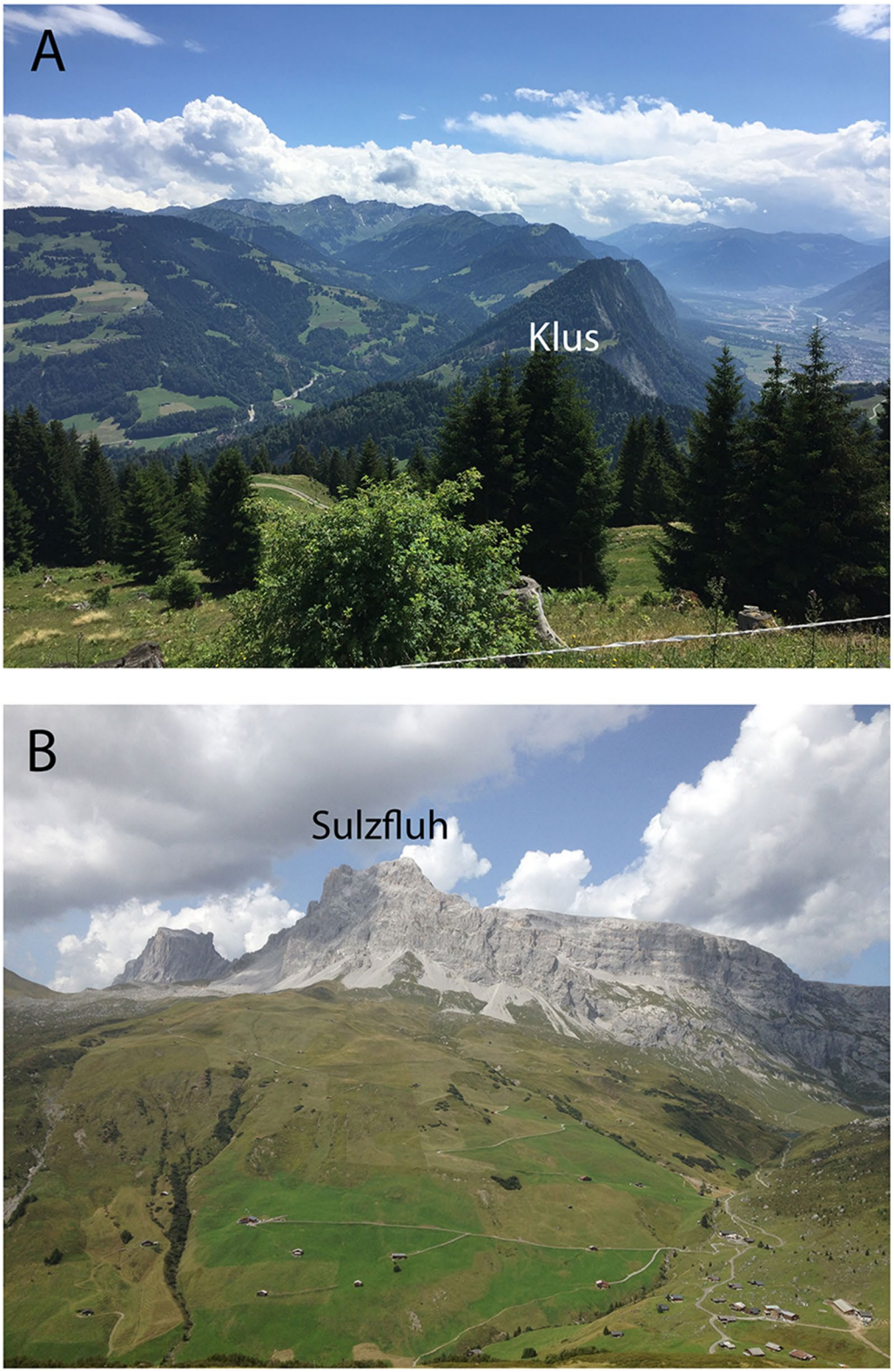

Fig. 3 Panoramic views of characteristic elements of the Prättigau half-window. **A** View from Vilanspitze to the south with the Rhine valley on the right and the Valzeina valley in the centre, separated from each other by the hard ridge of the Klus Formation. **B** View from St. Antönien to the north-west on the Middle Penninic Sulzfluh nappe framing the window (see also Fig. 4)

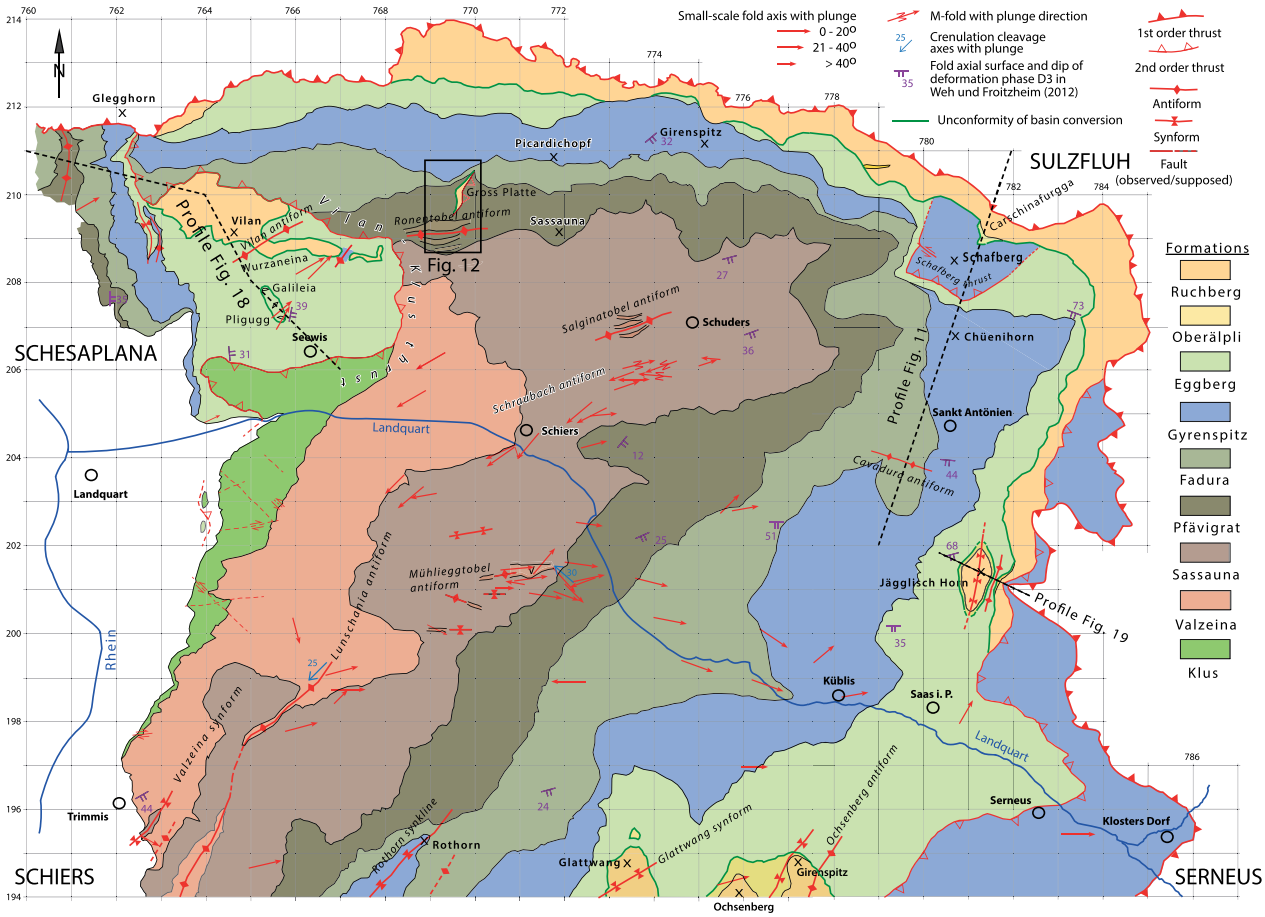

Fig. 4 Generalised map of the Bündnerschiefer and Flysch formations of the current mapping campaign on the Schesaplana, Sulzfluh, Schiers and Serneus sheets of the Swiss Geological Atlas. The map by Nänny (1948) was a useful basis, but had to be modified in several places. Some elements of the results of Steinmann (1994) and Weh and Froitzhein (2001) are integrated. Note the mapped unconformity (in green) between Cretaceous Bündnerschiefer and Cenozoic flysch formations and the variable order of thrusts along the eastern margin of the window

Alpes on top. Between the Middle Penninic and Australpine nappes, rocks of the South Penninic suture appear in variable thickness. This Arosa unit (Fig. 2) comprises mappable blocks and melange bodies of generally South Penninic and Lower Austroalpine origin (Bernoulli and Weissert, 1985, Lüdin, 1987, Winkler, 1988).

The North Pennic units and in particular those in the Prättigau half-window look back on a decades-long history of research. The presently utilised lithostratigraphic, respectively chronostratigraphic framework of the sedimentary formations goes back to Nänny (1948). This author unified and homogenized locally mapped lithostratigraphic units of earlier researchers (see Table 1 in Nänny 1948) into a coherent scheme that appears still valid today. However, puzzles remain, such as what the sedimentary basin fill is, what the triggering tectonic processes are, and how it fits with current basin conversion models.

In particular, we discuss the change from extensional to compressive basin tectonics in the North Penninic basins of eastern Switzerland. It is generally accepted that basin conversion initiates the formation of flysch and melange deposits during the Alpine orogeny, i.e., by the transition from extension to subduction and collision (e.g., Matter et al., 1980, Winkler, 1988, Caron et al., 1989, Gasinski et al., 1997, Pfiffner, 2014, p. 131). In addition, it is observed that in the Alpine Tethys realm conversion of basins and flysch deposition migrated in time from southern palaeogeographic realms (Cretaceous) to northern ones (Palaeogene) (Fig. 1) as depicted by time and space stepped flysch deposition (e.g., Trümpy, 1980). At the time of Nänny (1948), the dominant geosynclinal model demanded the Tethys-wide simultaneity of these tectono-sedimentary processes during the Cenomanian–Turonian. As a result, on various geological maps considering the Prättigau half-window the transition from

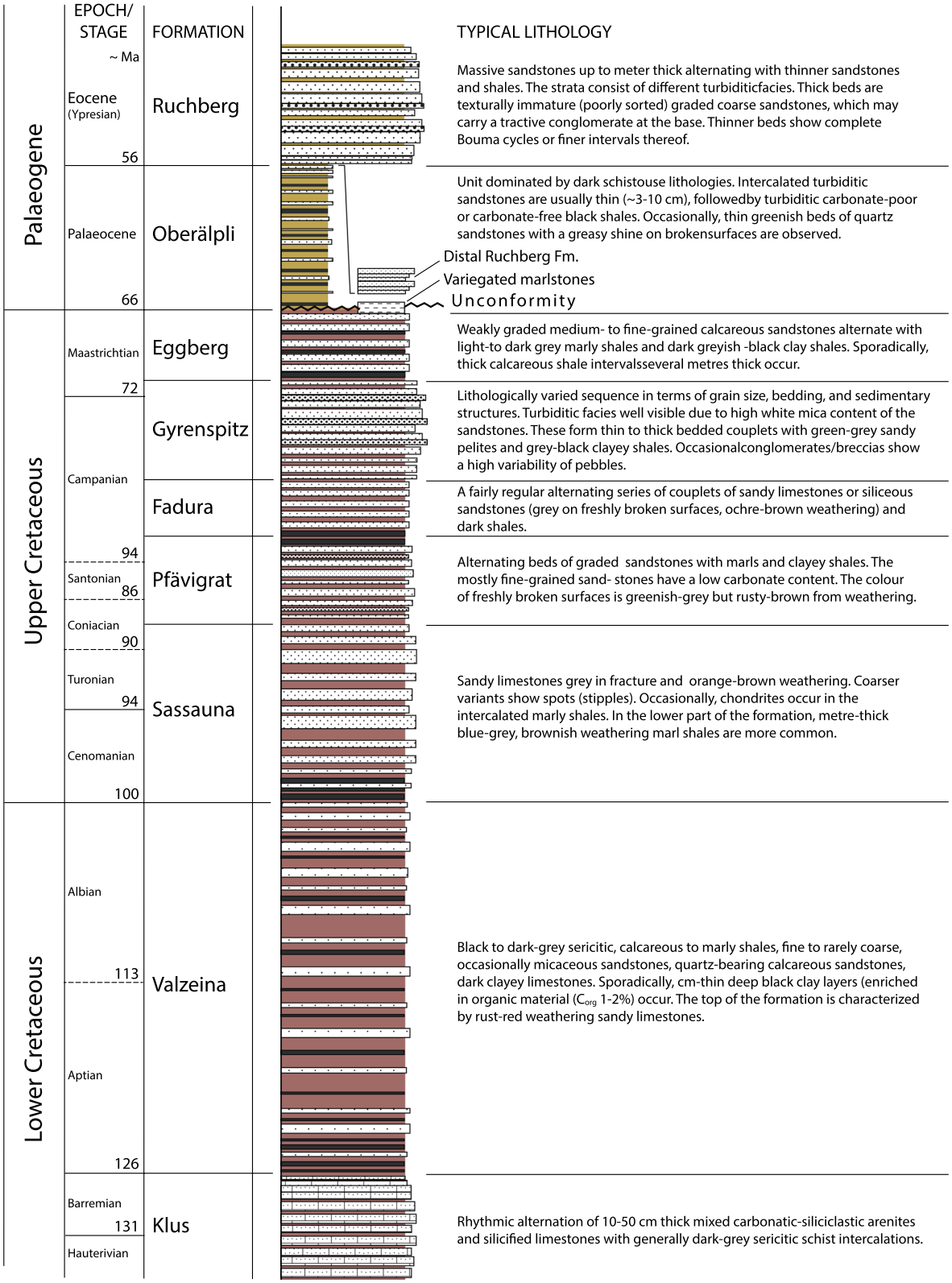

Fig. 5 Time-calibrated composite section of the Bündnerschiefer and Flysch formations in the Prättigau half-window. Chronostratigraphic scale after Gradstein et al. (2013)

Bündnerschiefer to Flysch is drawn at the base of the Turonian Pfävigrat Formation (Fig. 2), e.g., Bundesamt für Landestopografie *swisstopo* 2005, Steinmann, 1994).

The present study aims to unify older and new investigations in the sedimentary sequence of the Bündnerschiefer and Flysch series of the Prättigau and to develop a novel model for the tectono-stratigraphic evolution of the North Penninic realm of eastern Switzerland. The main reason for this rethink is our finding of an unconformity between Cretaceous and Palaeogene strata which implies a new reflection of the sedimentary and tectonic evolution of this part of the North Penninic basin.

2 Methods

In the frame of revising the Swiss Geological Atlas of the area of map sheets Schiers, Serneus, Schesaplana and Sulzluh were mapped at the scale of 1:10,000 (see a simplified summary in Fig. 4). Where possible, orientations of small-scale fold axes and bedding planes were measured. For describing the approximate modal composition of sandstones and biogenic content, partly feldspar and carbonate-stained thin sections were semi-quantitatively analyzed under the petrographic microscope. In representative sandstones from several formations, laser-ablation U–Pb dating of detrital zircons was applied. In the course of thin section study we discovered new micropalaentological evidence which were supported by M. Caron nd S. Spezzaferri (Univ. of Fribourg) and G. Coletti (Univ. Milano-Bicocca). In addition, the available rich data sets on metamophism and structures are integrated and referenced in the present report.

3 Lithostratigraphy and lithofacies

As mentioned above, the lithostratigraphic subdivision of the Bündnerschiefer and the Flysch, described by different authors in different areas of occurrence, was harmonized by Nänny (1948) in his time (Trümpy, 1916; Häfner 1924, Stahel, 1926, Blumental, 1931, Arni, 1933, 1935). The units are mainly distinguished by their bedding style and their proportions of carbonate and siliciclastic content (Fig. 5). Although it is not always easy to see, the turbiditic and hemipelagic facies are dominant in the formations. Earlier biostratigraphic calibrations were mainly provided by Arni (1933, 1935) and Nänny (1946, 1948) using foraminifers in coarser arenites. Due to intense post-depositional isoclinal folding, the thickness of the formations is difficult to estimate, but the entire formation stack originally could have measured about 1500 m and more.

According to recent geological mapping on the atlas sheets of Thusis (Wyss et al. 2017) and Reichenau (R. Wyss pers. comm. 2023), the Tomül nappe has a larger extent than previously assumed. Southwest of Chur (Fig. 2), the Grava nappe wedges out. Consequently, the sedimentary sequences of the Prättigau must be attributed to the Tomül nappe. However, over the long distance of 50–60 km of the N–S extension of this nappe, some lithological variations can be expected, which will also be described below where relevant.

3.1 Klus formation

The Klus Formation contains massive limestones and sandstones that make it a morphologically distinct feature characterised by high cliffs, such as the Klus Gorge shown in Fig. 3a. It contains a rhythmic alternation of 10–50 cm thick mixed carbonate-siliciclastic arenites and silicified limestones with generally dark-grey intercalations of sericitic shales (Fig. 6a). Limestones dominate the series. Grading in the beds is present but hardly to detect by eye. Microscopically, the beds are ferruginous spathic limestones with variable amounts of dispersed echinoid fragments and occasional layers rich in sponge needles (Fig. 7a). Dolomitic lithoclasts are present but rather rare. Pyrite nodules are common in places and detrital quartz grains show pressure shadows (fibrous beards) of phyllosilicates and quartz due to Alpine deformation.

Biostratigraphic correlation is lacking and the base of the sequence is not exposed (Nänny, 1948). The lower contacts are all of tectonic (thrust) character (Fig. 4). Based on indirect stratigraphic arguments, the formation can be correlated with the pre-Aptian, probably Hauterivian-Barremian, because the Valzeina Formation overlying the Klus Formation correlates with the Nollaton Formation in the Tomül nappe.The latter was calibrated as Aptian-Albian by means of Neodymium isotope geochemistry and regional lithologic comparisons (Steinmann 1994).

The probably coeval Bärenhorn Formation in the southern part of the Tomül nappe (Steinmann 1994) is lithologically more variable, with mixed quartz and calcarenites, dark limestones and quartz-rich sandstones. The formation overlies the prasinites of the Tomül "greenstone succession" (Steinmann 1994, and references therein).

3.2 Valzeina formation

The unit has a thin-bedded, monotonous appearance. However, it is more varied in detail. In the lower part, shiny grey-black shales dominate which sporadically bear intercalations of cm-dm thin sandy limestones. There is a rhythmic succession of black to dark grey sericitic, calcareous to marly shales (Fig. 6b), fine to rarely coarse, sometimes micaceous sandstones, quartz-bearing calcareous sandstones, dark clayey limestones. Occasionally,

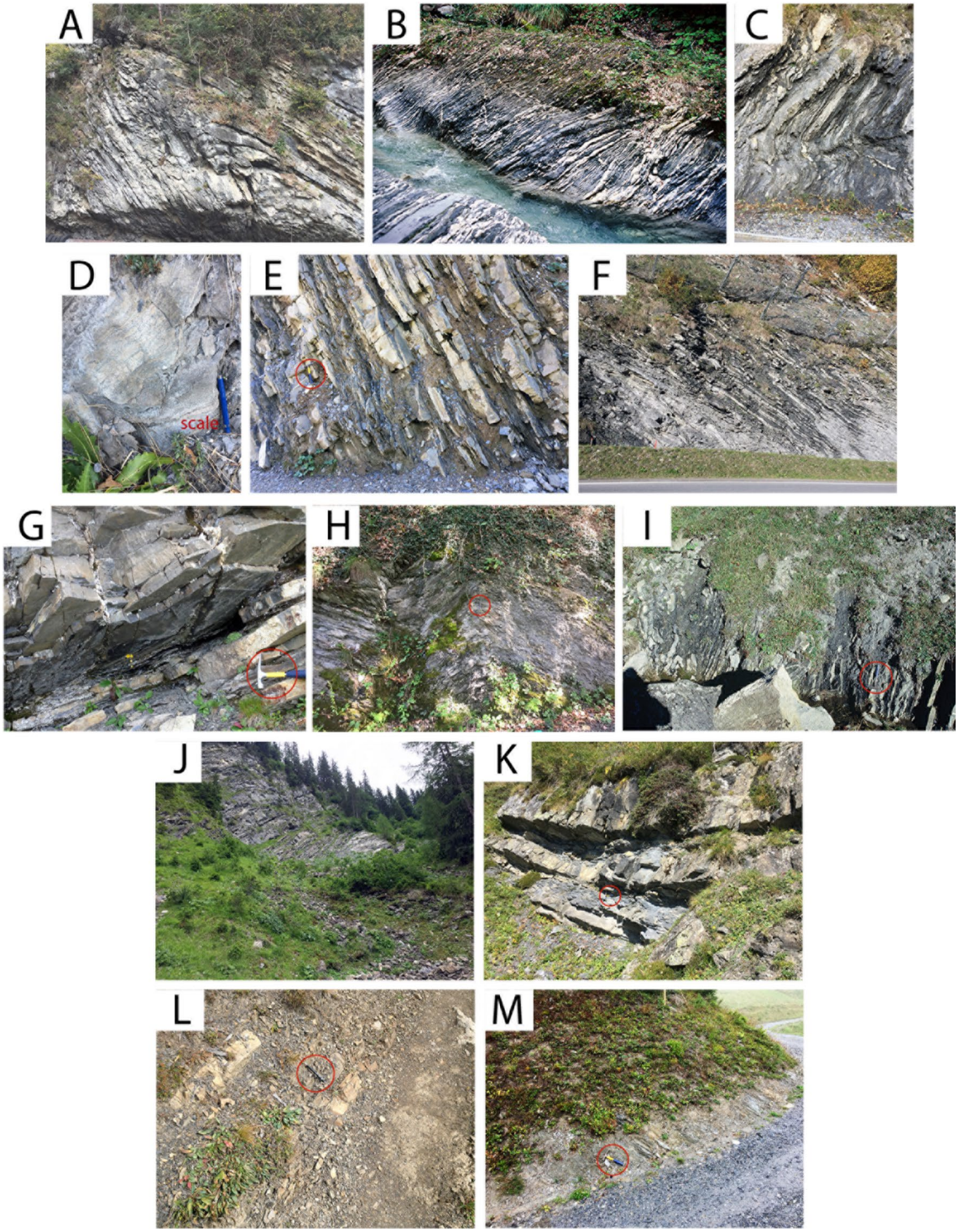

Fig. 6 Field photos of selected outcrops showing the lithological characteristics of the formations. **A** Klus Fm. **B** Valzeina Fm. **C** folded and kinked Sassauna Fm. **D** Coarse Sassauna Fm. showing the so-called "Tüpfelschiefer". **E** Regularly bedded Pfävigrat Fm. **F** Fadura Fm. **G** thick-bedded Gyrenspitz Fm. with upward younging. **H** intensely folded Eggberg Fm. also showing pencil structures. **I** subvertically bedded Oberälpli Fm. in the Chrützböden locality, from which most of the new biostratigraphic results of the formation were obtained. **J** massive Ruchberg Fm. sandstone unconformably overlying Pfävigrat Fm. sandstone. **K** classical outcrop of the Ruchberg Fm. in the northern flank of the Ruchberg. **L** laminated thin-bedded (distal) Ruchberg Fm. in the Chläsi locality. **M** variegated marls probably overlying the Egberg Fm, nannoplankton results indicate a Maastrichtian or younger age (written comm. Eric de Kaenel 2020)

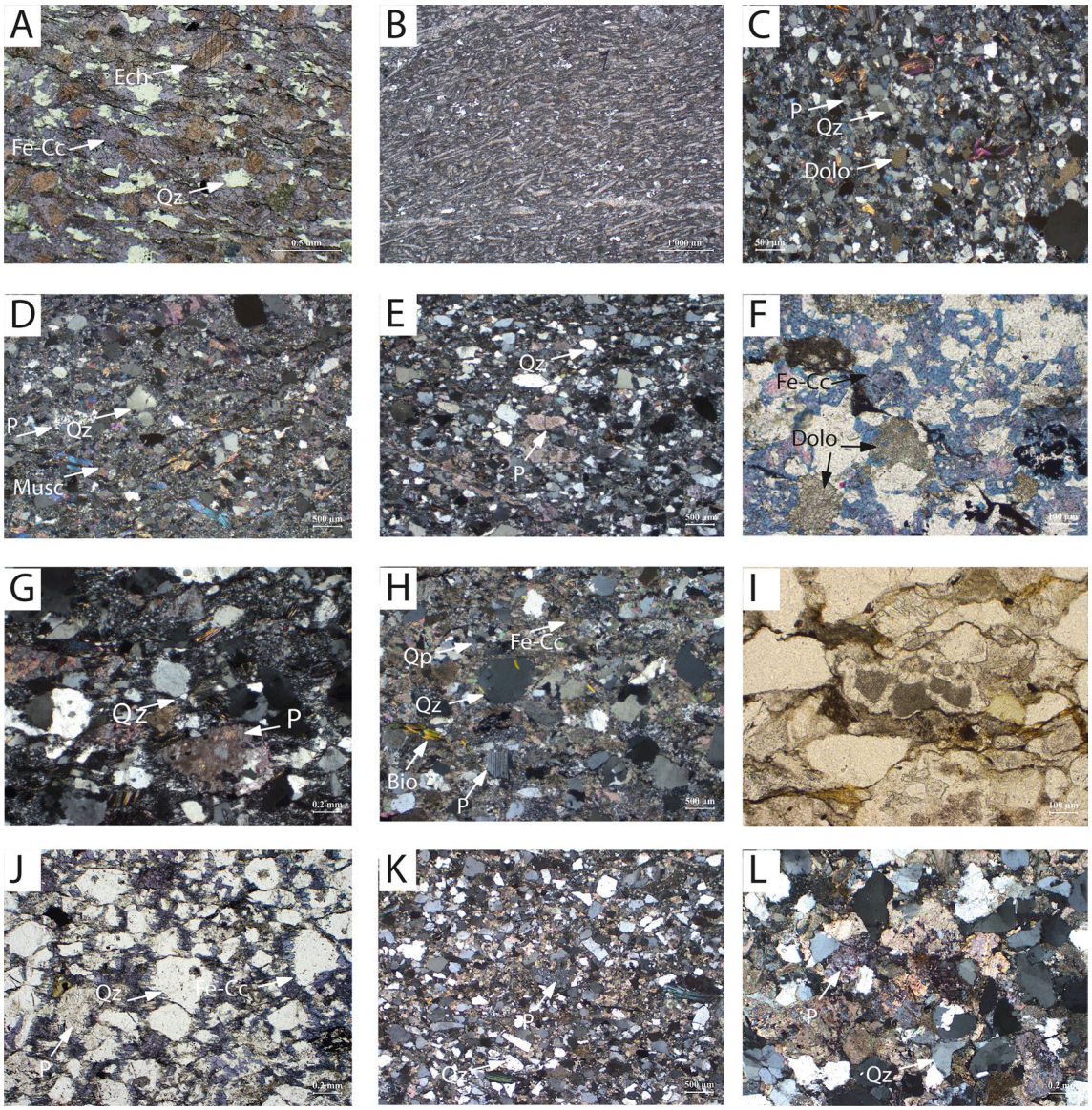

Fig. 7 Microphotos of thin sections. Note that as few metamorphic or sheared examples as possible are shown. *Qz* quartz, *Qp* polycrystalline quartz, *P* plagioclase, *Musc* muscovite, *Bio* biotite, *Dolo* dolomite lithoklast, *Ech* Echinoderm fragment, *Fe-Cc* iron-bearing calcite. **A** Quartz-bearing limestone bed of the Klus Formation; thin section stained for carbonate under normal light; echinoderm fragments (brownish-red) in iron-bearing sparitic calcite cement (blue); uncoloured grains are corroded quartz. **B** Spongy limestone from the Klus Formation under normal light. **C** Relatively coarse-grained sandstone from the Valzeina Formation (+ Nicols) consisting of quartz, plagioclase and muscovite; brownish grains are dolomite clasts. **D** Coarse sandstone in the lower part of the Sassauna Formation; besides quartz and corroded plagioclase, the calcite-cemented sandstone is rich in muscovite; + Nicols. **E** Thin section stained for feldspars from the Pfävigrat Formation; + Nicols; pinkish plagioclase is visible next to dominant quartz. **F** Carbonate-stained sandstone from the Pfävigrat Formation with similar characteristics as shown in **A**; here brownish-grey fine-sparitic to micritic dolomite lithoclasts can be seen. **G** Coarse arkose sandstone coloured for feldspars from the Fadura Formation; polarised light; plagioclase appears greyish pink, quartz is uncoloured; the matrix is siliceous and an incipient formation of fibrous beards is visible in the pressure shadows of the quartz grains. **H** Sublitharenite from the Gyrenspitz Formation; quartz dominates among the terrigenous grains, plagioclase and polycrystalline lithoclasts make up about 10% each; sparitic ferruginous cement; + Nicols. **I** Globotruncana *linneiana* in a sandstone of the Gyrenspitz Formation (pers. comm. M. Caron, Université de Fribourg, 2021). **J** Arkose from the Eggberg Formation, stained for carbonate under normal light; ferrous calcite cement (blue) and fibrous beards in the pressure shadows of the quartz grains. **K** Subarkose from the upper part of Oberälpli Formation; + Nicols. **L** Quartz-rich feldspathic litharenite of the Ruchberg Formation; stained for feldspar and under crossed Nicols. Quartz grains (grey to white) and plagioclase (pink) embedded in sparitic calcite cement

cm-thin deep black clay layers (enriched in organic material, C_{org} 1–2%, WW unpublished data) occur. The sandy limestone layers often show boudinage, which also turn out to be small fold hinges when they are broken up. On the whole, a coarsening of the detritus towards the top of the formation is observed. In the upper part in the area of the transition to the overlying Sassauna Formation, the occurrence of 2–20 cm bedded rust-red weathered, dark grey sandy limestones is noted. However, over all, shales dominate the formation with 70–80%.

In thin section, the fine sandy/siliceous limestones are strongly schistose and the fine ferruginous sparitic calcite cement dominates with about 50–60%. Quartz grains are almost always recrystallised or show jagged cross-sections. Muscovite occurs in proportions of 3–10%. Detrital plagioclase can rarely be observed, whereas diagenetic albite frequently occurs; pyrite cubes and globules are characteristic in cement and stylolites. In less deformed samples, in decreasing abundance detrital angular to edge-rounded quartz, plagioclase, muscovite and dolomite lithoclasts are observed. Echinoderm fragments are present in the lower part of the formation. These are also typical for the underlying Klus Formation.

In inner parts of the Tomül nappe, the same rock sequence is called Nollaton Formation and is assigned an Aptien-Albian age by Steinmann (1994, and references therein). This has been demonstrated by the author through transregional comparisons with similar Lower Cretaceous formations and Neodymium geochemical systematics. Both occurrences show a several metre thick interval of rust-brown sandstone beds at the transition to the younger formation (Sassauna respectively Nollakalk Formations) (Steinmann 1994).

3.3 Sassauna formation

In general, this unit contains more or less regular repetitions (dm-m scale) of sandy limestones and marly to argillaceous shales (Fig. 6c). The transition from the underlying Valzeina Formation is well exposed in various outcrops. It is defined by the occurrence of alternating regularly bedded siliceous limestones and grey to black shales above the rust-red weathered sandy limestones attributed to the top of the Valzeina Formation. Of note is the increased content of white mica or sericite in the Sassauna Formation, which gives a silvery lustre to the bed surfaces.

Orange weathered marly slates partly occur in metric beds and have a blue-grey fracture colour. The sandy limestones are grey in fracture and orange-brown in weathered; coarser varieties show stippling, which Nänny (1948) identified as pigment-rich lime grains ("Tüpfelschiefer", Fig. 6d). Occasionally chondrites or sole marks occur in the marly shales or at the base of the sandy limestones. In the lower part of the formation, the above-mentioned metre-thick blue-grey, brownish weathered marly shales are more common.

Depending on the degree of tectono-metamorphic overprinting, the components of the sandy limestones are better or worse preserved Fig. 7d). In the former case, they contain about 50–60% extrabasinal grains (in descending order quartz, plagioclase, muscovite, dolomite lithoclasts), 10–20% bioclasts (mostly echinoderm fragments, minor bryozoans and benthic *foraminifera*) in ~30% sparitic Fe-bearing calcite cement. Syntaxial cement overgrows the echinoderm fragments. Based on the extrabasinal grains, the rock is classified as subarkose. With stronger metamorphic overprinting, reticular stylolitisation occurs, quartz is strongly corroded at the margins, plagioclase becomes scarce and diagenetic albite is formed. Muscovite flakes remain unaffected.

Earlier research and the present one could not provide biostratigraphic material for an age correlation. Only a relative age can be deduced from the age interpretations of the underlying and overlying formations. This age is thought to be Cenomanian to Coniacian.

Using the above methods, Steinmann (1994) determined a Cenomanian age for the correlatable Nollakalk Formation in the inner parts of the Tomül nappe. It consists of quartz-bearing limestone beds with occasional gradations. A general thinning trend of the beds with a correlative increase in dark shales is described by Steinmann (1994). The orange to light grey weathering of the rocks is also similar.

3.4 Pfävigrat formation

The Pfävigrat Formation is made up of alternating beds of sandstones, marls and clayey shales. The generally fine-grained sandstones have a low carbonate content. The colour is greenish-grey on freshly broken surfaces, but rusty-brown from weathering. Typically, the graded sandstone beds are overlain by greenish-grey marls and greenish-black clays, i.e., they represent turbiditic beds. At the base, the unit is thin-bedded and platy (Fig. 6e) in the range of a few dm; sporadically thicker metric ones are intercalated. Pelitic calcareous beds rarely occur. The sandstones are rich in white mica, and dolomite lithoclasts are not rare. Chondrites and other traces of activity are found on the base of beds. Shiny sericite schists are observed in more metamorphically overprinted segments. Then, crenulation schistosity becomes visible. As reported by Nänny (1948), breccias and conglomerates are present in the formation in the northern part of the Prättigau window, carrying crystalline basement and dolostone pebbles.

The lithological boundary to the underlying Sassauna Formation is difficult to define due to the paucity of

suitable outcrops and the intense internal deformation and folding of the formation boundary. In some outcrops, a dark shale interval tens of metres thick forms the top of the Sassauna Formation. The base of the Pfävigrat Formation is defined by the first occurrence of sandstones.

In thin section (Fig. 7e, f), the sandstones show contents of quartz (40–60%), plagioclase (20–40%), mostly white mica (3–5%), subordinate rock fragments (mostly dolomite, polycrystalline quartz) and partly abundant bioclasts (up to 20% echinoderms, bryozoans, partly silicified planktic and benthic *foraminifera*, inocerams). The groundmass consists of iron-bearing sparitic calcite-cement amounting ca. 30% of the total rock. Under stronger metamorphic overprint, the sandstones show intense silicification and recrystallisation. The sandstones of the Pfävigrat Formation are classified as lithic arkoses and feldspathic litharenites.

Regarding the biostratigraphic age classification of the Pfävigrat Formation, Nänny (1948) determined according to current taxonomy rules (Young et al. 2017) the planktic *foraminifera Globotruncana lapparenti*, *G. bulloides*, *Marginaotruncana renzi*, *Praeglobotruncana stephani* and *Thalmanniella appenninica*. In our thin sections, M. Caron (pers. comm., 2021) in addition identified *Rotalipora monsalvensis*, *Praeglobotruncana gibba*, *Globotruncana linneiana, Rotalipora* sp. *Ticinella* sp. *Marginotruncana* sp. Considering the first appearance of species, as recommended in turbidite series, *G. lapparenti* and *G. bulloides* would indicate an age of early-middle Coniacian and younger. Nevertheless, a start of deposition in the Turonian seems possible.

With regard to uncertain age calibrations in the inner Tomül nappe, the correlative formation should be the Carnusa Formation and the so-called "Hauptkonglomerat" (Main conglomerate, Jäckli, 1941; Steinmann, 1994; Burla, 1997). Further south, in the Tomül nappe in the Hinterrhein area, limestone facies (including the morphologically prominent 'Safier Limestone' and intraformational matrix-supported conglomerates) are more common. However, Steinmann (1994) and Burla (1997) describe a northward and stratigraphically younging trend of increasing terrigenous content and grain size, the latter being manifested by conglomeratic intercalations culminating in the Main conglomerate.

This member is thought to represent the lowest part of the so-called Tomül Flysch (Jäckli 1941, Steinmann 1994). In the Stätzerhorn area, Burla (1997) summarized the overlying turbiditic formations in the ca. 1500 m thick Stätzerhorn Group. No age data are available. Lithostratigraphic similarity with younger formations in the Prättigau is not obvious, but this may be due to basin-wide lateral facies variations caused by basin and detrital source dynamics. However, Paleogene formations are not known to have existed.

3.5 Fadura formation

This unit is marked by a fairly regular alternating series of couplets of sandy limestones or siliceous sandstones (grey on freshly broken surfaces, weathered ochre-brown) and dark shales (Fig. 6e). In detail, these dm-scale (10–30 cm) couplets consist of a hard beds overlain by calcareous blue-grey pelites (often parallel laminated and chondrite-bearing) and green-grey to black clays. Fine muscovite is enriched in the sandy beds and especially in the parallel laminated pelites. Small millimetric dolomite clasts are recognized as orange dots. This typical regular alternating bedding is occasionally interrupted by thick (0.5–1 m) black carbonate-poor clayey shale intervals. The boundary with the underlying Pfävigrat Formation can only be approximated due to unfavourable outcrop conditions and Quaternary cover. According to our observations, the upper part of the Pfävigrat Formation shows in places an irregular alternation of sandstones and sericitised (glossy) shales, the latter increasing in thickness. For practical reasons, the base of the Fadura Formation is drawn where the typical regular thin sandstone-shale pairs occur.

Thin sections of the sandstone beds show a twofold character. Most common are sandy limestones with contents (Fig. 7g) of, in decreasing frequency, quartz (mosaic recrystallised), plagioclase, white mica, dolomite grains and few recrystallised bioclasts. These detrital grains are embedded in Fe-bearing calcite cement in which pyrite grains also float. Nänny (1948) mentioned finds of bryozoans, inoceramid detritus, textularia, spongy needles and globotruncanids. Their preservation depends strongly on the variable tectono-metamorphic overprinting. According to the terrigenous detritus, they are quartz-rich arkoses. The other type of sandstones carries a siliceous-clayey matrix in grain-supported (ca. 30%) and matrix-supported (ca. 50%) texture. The greater variability of the lithoclasts is another distinguishing feature. In decreasing frequency of terrigenous grains, quartz, plagioclase, lithoclasts and white mica are observed. The lithoclasts include finely textured polycrystalline and tectonized quartz, quartz phyllites, granitoids, volcanics, sandstone and minor dolomite. Echinoderm fragments are almost completely absent or have been eliminated by recrystallisation. The proportions of terrigenous grains

and nodules classify the latter sandstones as lithic arkoses and feldspar-bearing litharenites.

Despite the paucity of biostratigraphic data, the presence of *Globotruncana lapparenti* and some subspecies described by Nänny (1948) suggests a Santonian to Campanian age.

3.6 Gyrenspitz formation

The Gyrenspitz Formation is a lithologically varied sequence in terms of grain size, bedding, and sedimentary structures. The turbiditic facies is evident from gradational, parallel, rippled, and convolute layering in the sandstones and pelites (5f, g). The sandstones are medium grey in fracture and have an ochre-brownish weathering. Thin-bedded sandstone layers (about 20–30 cm thick) typically have a sandy base that passes into green-grey sandy pelites and is finally topped by grey-black clayey shales. In these facies the pelites can also dominate. Intercalated in this basic matrix are bundles of thicker turbidite cycles, which consist of up to few meter-thick cycles that show vertical coarsening/thickening or fining/thinning. Conglomerates/breccias (pebble size 3–10 cm), massive coarse sandstones, amalgamations (welded bedding) and slumps occur in such bundles. In the sandstones, intrabasinal pelitic mud flakes also occur, and chondrites and helminthoids are not uncommon in the fine layers. Also, metric blue–grey weathered turbiditic pelites occur, which carry a thin sandstone base.

The contact with the underlying Fadura Formation is rarely exposed. The boundary is drawn where the regular alternation of sandy limestones and marly shales of the Fadura Formation are replaced by initially thin and irregularly bedded sandstones alternating with marly shales and green-grey to black clayey shales. Over a few 10 m the sandstones become thicker, indicating a progradational trend.

Visual estimation of grain types in thin section classifies the sandstones as feldspar-bearing litharenites. Rock fragments encountered are dolomites, bioclastic

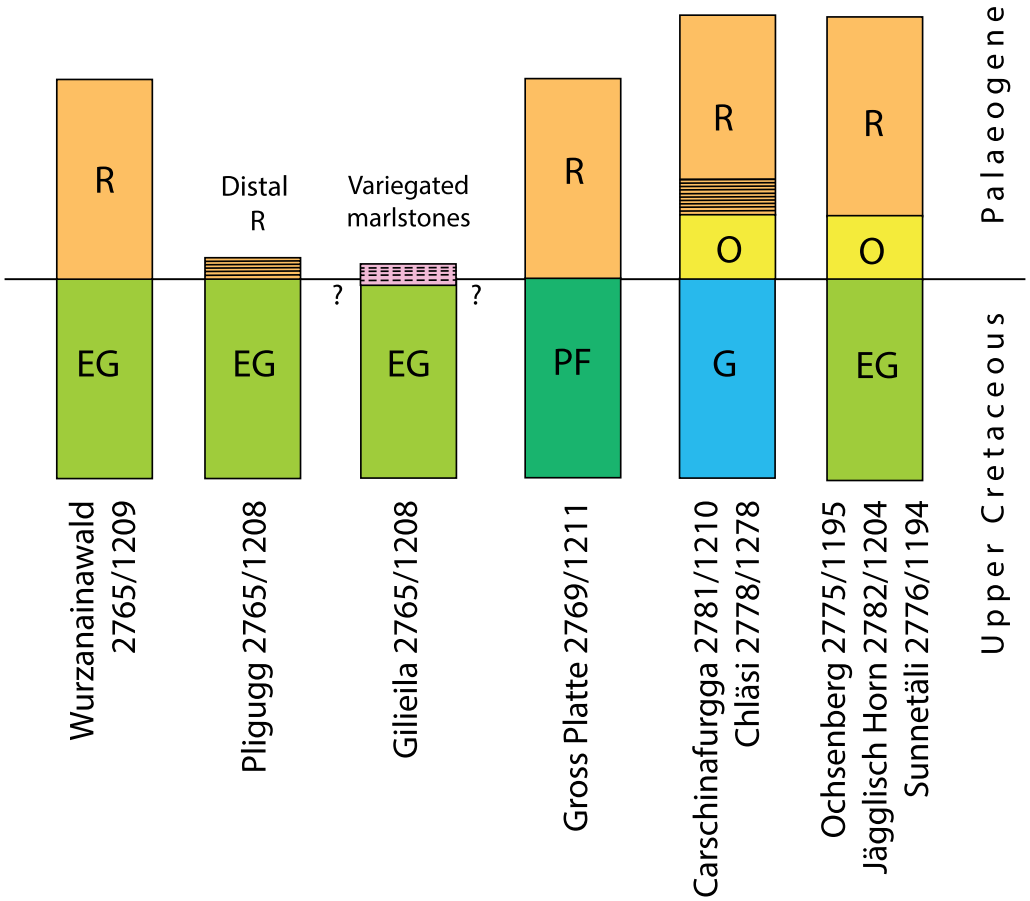

Fig. 8 Schematic representation of the mapped contacts between Bündnerschiefer and Flysch in the northern Prättigau half-window at various localities. The chronostratigraphic position of the variegated marls is still under discussion. Formation abbreviations: EG, Eggberg; G, Gyrenspitz; O, Oberälpli; PF, Pfävigrat; R, Ruchberg. In addition, the final numbers of the locations in Swiss Grid Coordinates

Fig. 9 Left: Looking east from Ochsenberg over Girenspitz and Sunnentäli. It shows slightly folded Oberälpli (O) and Ruchberg (R) formations with NE plunging fold axes. On the right: View on a slipped block of Pfävigrat Fm. in the area of the Lunschania antiform showing crenulation cleavage. See also Fig. 4

limestones, spathic limestones, volcanites, phyllites, gneisses, calpionella-bearing micritic limestones, cherts, sandstones, and graphitic sandstones. Muscovite and biotite are present in smaller amounts (2–5%). A similar value is attributed to echinoderm fragments. The cement is consistently iron-bearing calcite in fine and coarse sparitic form. With stronger tectono-metamorphic overprinting, silicification and growth of fibrous beards in pressure shadows on detrital quartz occur. Glauconite is preserved in small amounts, but metamorphically bleached light green. In breccias, the abundance of micritic calcareous pebbles with recrystallized radiolarians, calpionellidae, filaments and *foraminifera* as well as red marly limestones is striking. This occurrence suggests that part of the supply came from the area of the Middle Penninic (Sub-Briançonais). In addition, there are fragments of granitoids. The polygenic nature clearly distinguishes the Gyrenspitz Formation from the older units.

According to the taxonomic practice of planktonic *foraminifera* in use today, *Globotruncana lapparenti*, *G. neotricarinata*, *G. tricarinata desoi, G. linaeana*, and *G. arca* were found by Nänny (1948) and indicate a Santonian formation age and younger (Young et al., 2017, Boudaugher-Fadel, 2018). However, the occurrence of *Orbitoides media* finally points to a Campanian age (e.g., Baumfalk and Van Hinte (1985).

3.7 Eggberg formation

Lithologically, the Eggberg Formation is irregularly bedded in the upper dm range. It shows pronounced isoclinal folding with boudinage (Fig. 6h). The weakly graded hard beds alternate with light to dark grey marl shales and dark grey to black clayey shales. Isolated isoclinally folded intervals of calcareous shale are several metres thick. The hard beds are medium- to fine-grained calcareous sandstones with variable quartz and muscovite contents and dolomite grains. The sandstones have a spathic lustre due to the presence of coarse-grained calcite cement. Coarse sandstones and breccias are rare.

The contact with the underlying Gyrenspitz Formation is rarely exposed. In few places, above irregularly bedded brown weathered sandstones and marly shales of the Gyrenspitz Formation follows an interval of platy sandy limestones in carbonate-bearing black shales several metres thick. The thickness and grain size of the quartz-bearing limestones then increases (to 10–20 cm). The lower limit of the Eggberg Formation would thus be defined where the typical sandstones of the Gyrenspitz Formation end and are replaced by thicker calcareous shales and sandy limestones.

Under the microscope, the detrital grains are embedded in ferrous calcite cement (15–20%) and, with stronger tectono-metamorphic overprinting, mosaic-like silicification and the formation of fibred beards in the pressure shadow of quartz grains. Occasionally, up to 10% diagenetic dolomite rhombohedra occur. Biogenic detritus (mainly echinoderm fragments) makes up 5–10% of the total rock. Nänny (1948) reported also the presence of bryozoans, inoceramid fragments, spongy needles, and benthic *foraminifera*. Quartz, plagioclase, dolomite lithoclasts and white mica are observed in decreasing frequency. Dolomitic lithoclasts show both micritic and

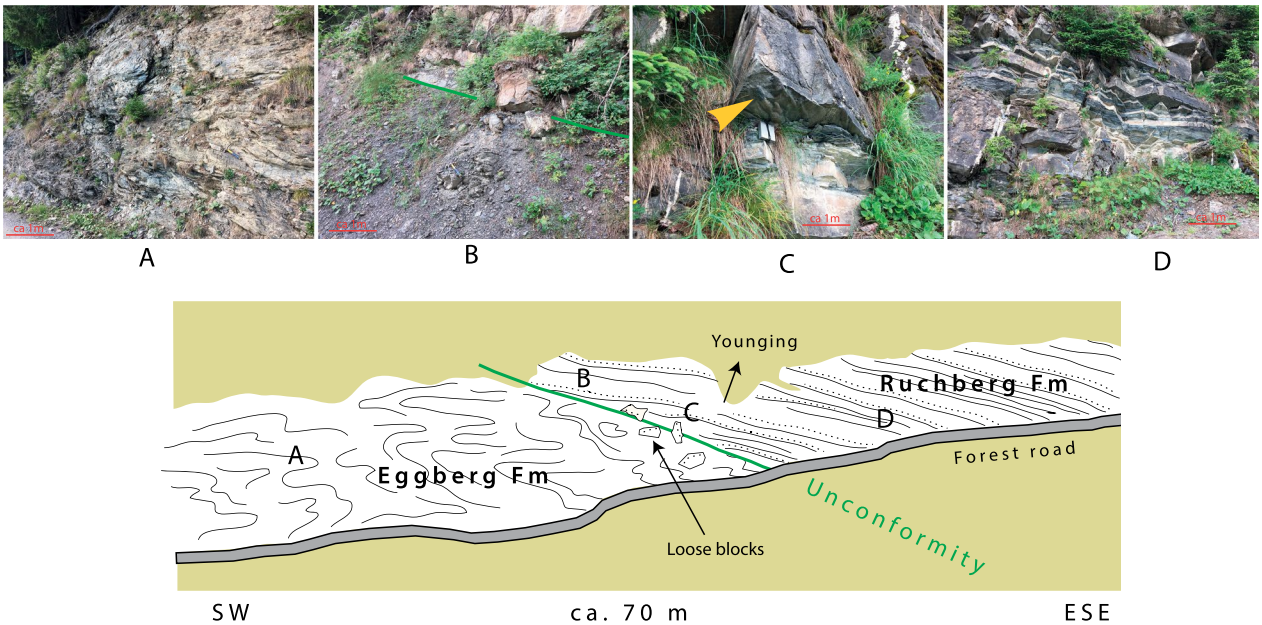

Fig.10 Coherent and normally bedded Ruchberg Formation in the Wurzaneina Forest (Swiss Grid Coord. 2766.635/1208.620). It unconformably overlies the folded and cleaved, anchizonally metamorphosed Eggberg Formation. Details are shown in photos **A**–**D**. A flow mark is visible in photo C, indicating south to north transport. The scale hammer is circled in red

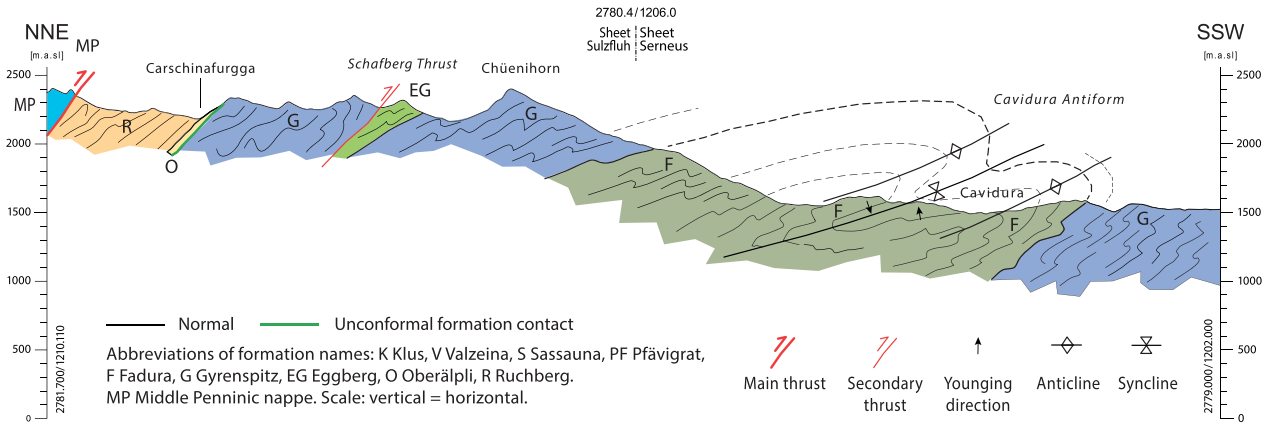

Fig. 11 Geological profile from Carschinafurgga to Cavidura Alpe. See Fig. 4 for location

sparitic textures. According to the abundance of terrigenous grains, the sandy limestones are classified as lithic arkoses and feldspathic litharenites.

According to the taxonomy of planktonic *foraminifera* in use today, *Globotruncana stuarti* found by Nänny (1948) is the youngest form of all planktic *foraminifera* mentioned by him and indicates a formation age of Maastrichtian and younger (Young et al. 2017, Boudaugher-Fadel 2018).

3.8 Oberälpli formation

The unit is dominated by dark shaly lithologies. Interbedded turbiditic sandstones are typically 3–10 cm thick, followed by turbiditic carbonate-poor or carbonate-free black shales (Fig. 6i). Sporadic thin green-grey clayey shales are also present between these cycles. Occasionally, thin greenish beds of quartz sandstones with a greasy shine on broken surfaces (vulgo "Ölquarzite") occur. As already noted by Nänny (1948), the Oberälpli Formation shows a restricted pattern of occurrence (Fig. 4).

In thin sections, the binder is 20–40% feerrous calcite cement in which the terrigenous grains and bioclasts are arranged in a grain-supported fabric. In decreasing abundance, these are quartz, plagioclase, mica (muscovite and less frequently chlorite) grains, and about equal numbers of lithoclasts (dolomite, polygenic and tectonic quartz). Echinoderm fragments dominate the bioclastic detritus, planktonic/benthonic foraminifers occur in some sandstones. Stylolites and pyrite nodules occur as diagenetic products, with clustered dolomite rhomboids in individual samples.

During our mapping, the contact with the underlying Eggberg Formation could not be observed. Theoretically, it should be drawn where black marly shale layers become dominant and possibly beds of greenish quartz sandstones ("Ölquarzite") occur. Due to its composition and position between the Eggberg and Ruchberg formations, a Palaeocene age was inferred (Nänny, 1948). In a quite fossil rich sandstone from the Kreuzboden locality, Silvia Spezzaferri (pers. comm. 2022) amongst fragments of *Morozovella* ssp. recognised *Chiloguembelina* sp., *Praemorica inconstans*, *Praemurica* cf. *uncinata*, *Acaranina* cf. *strabocella*, *Igorina* cf. *pusilla* and a specimen of *Parasubbottina pseudobulloides*. This faunal

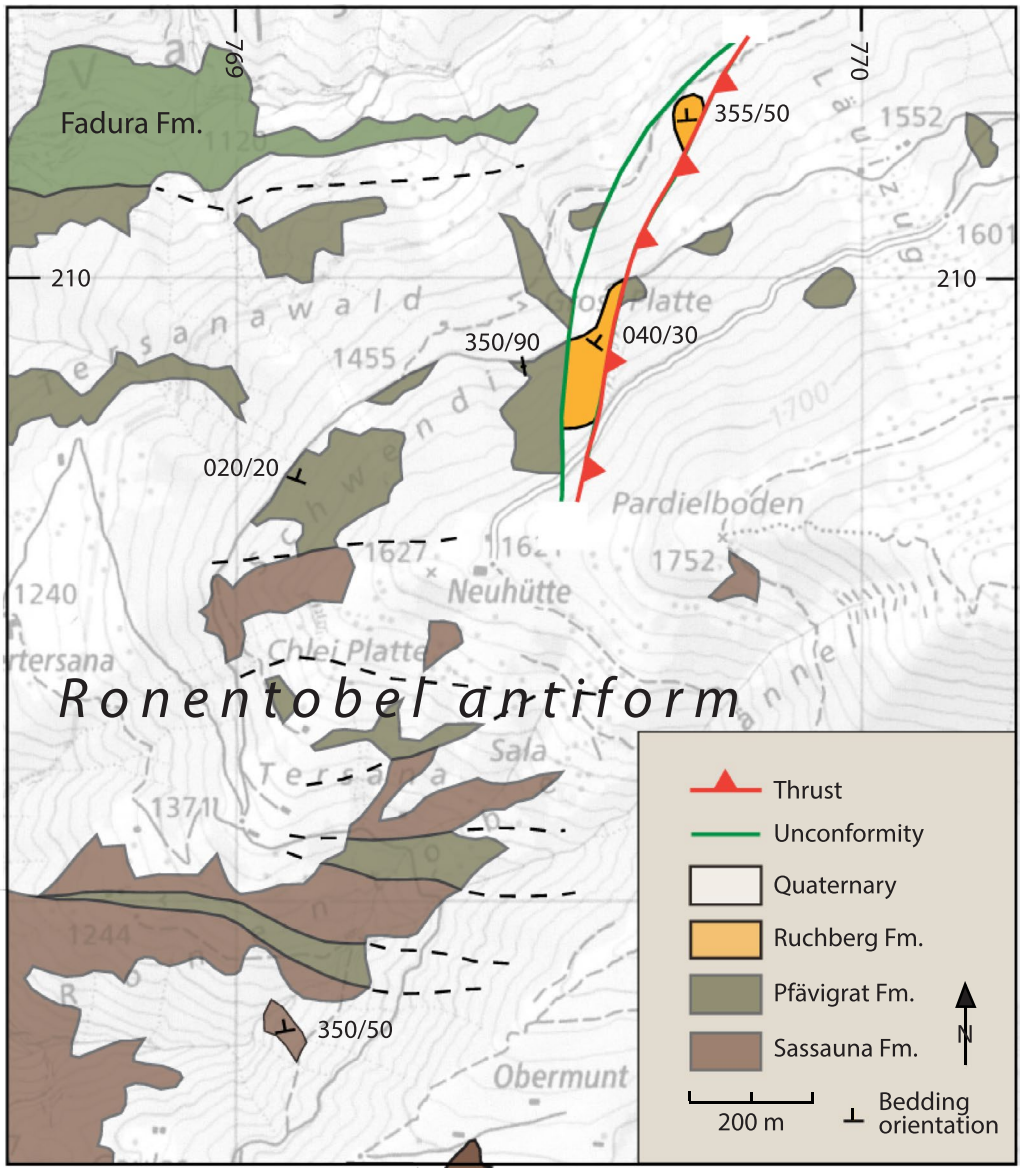

Fig. 12 Detailed map of the Ronentobel area and the Gross Platte site, showing the wedge of the Ruchberg Sandstone Formation unconformably overlying and later thrusted by the Pfavigrat Formation. See Fig. 4 for location and field photo Fig. 6j

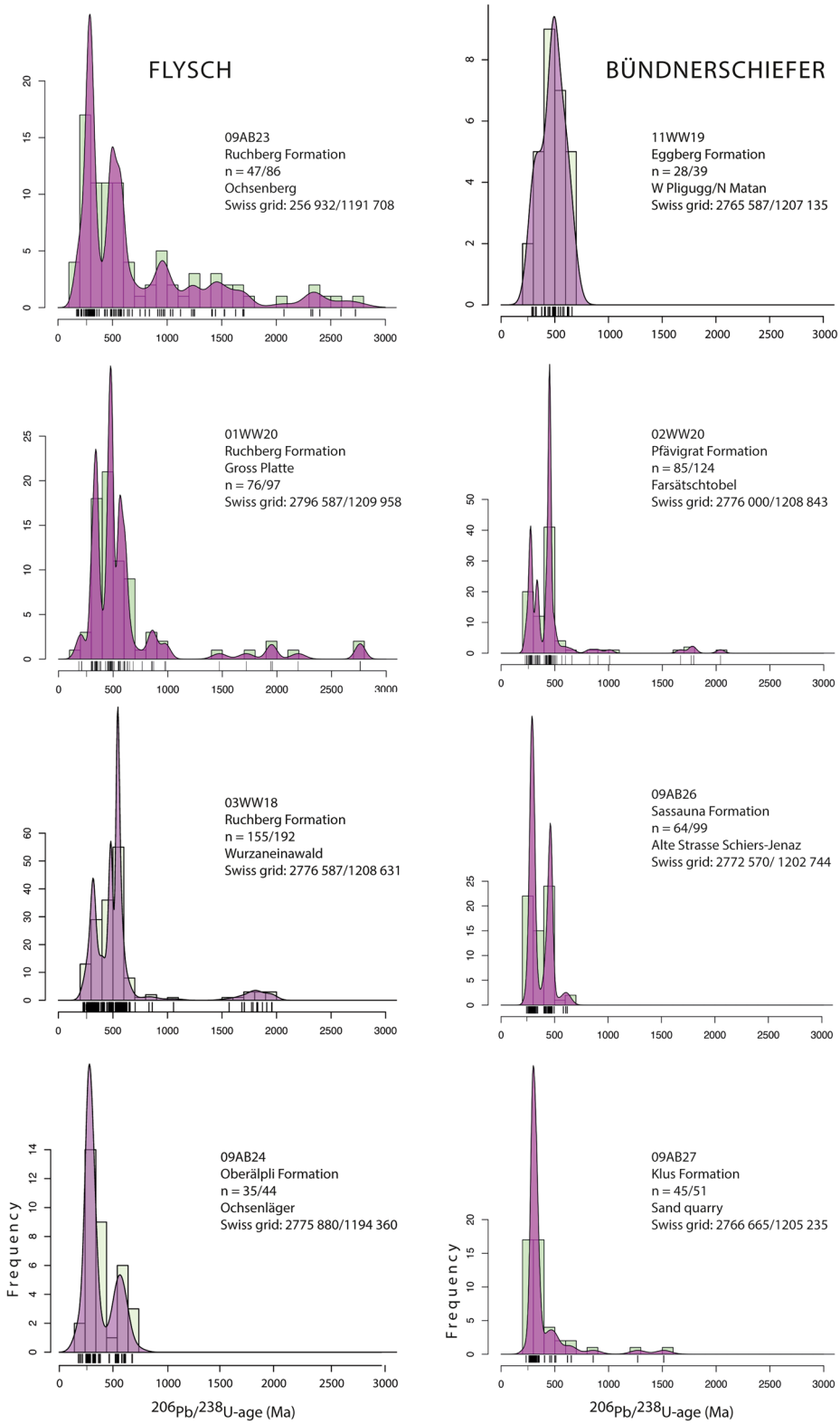

Fig. 13 U–Pb age spectra of detrital zircons in Bündnerschiefer (right row) and Flysch (left row) formations in the North Penninic of the northern Prättigau half-window. Kernel density estimates (KDE) after Vermeesch (2018). Only concordant ages were selected, expressed as the ratio n = concordant/total age measurements. LA-ICP-MS measurements carried out at the Institute of Geochemistry and Petrology, ETH Zurich

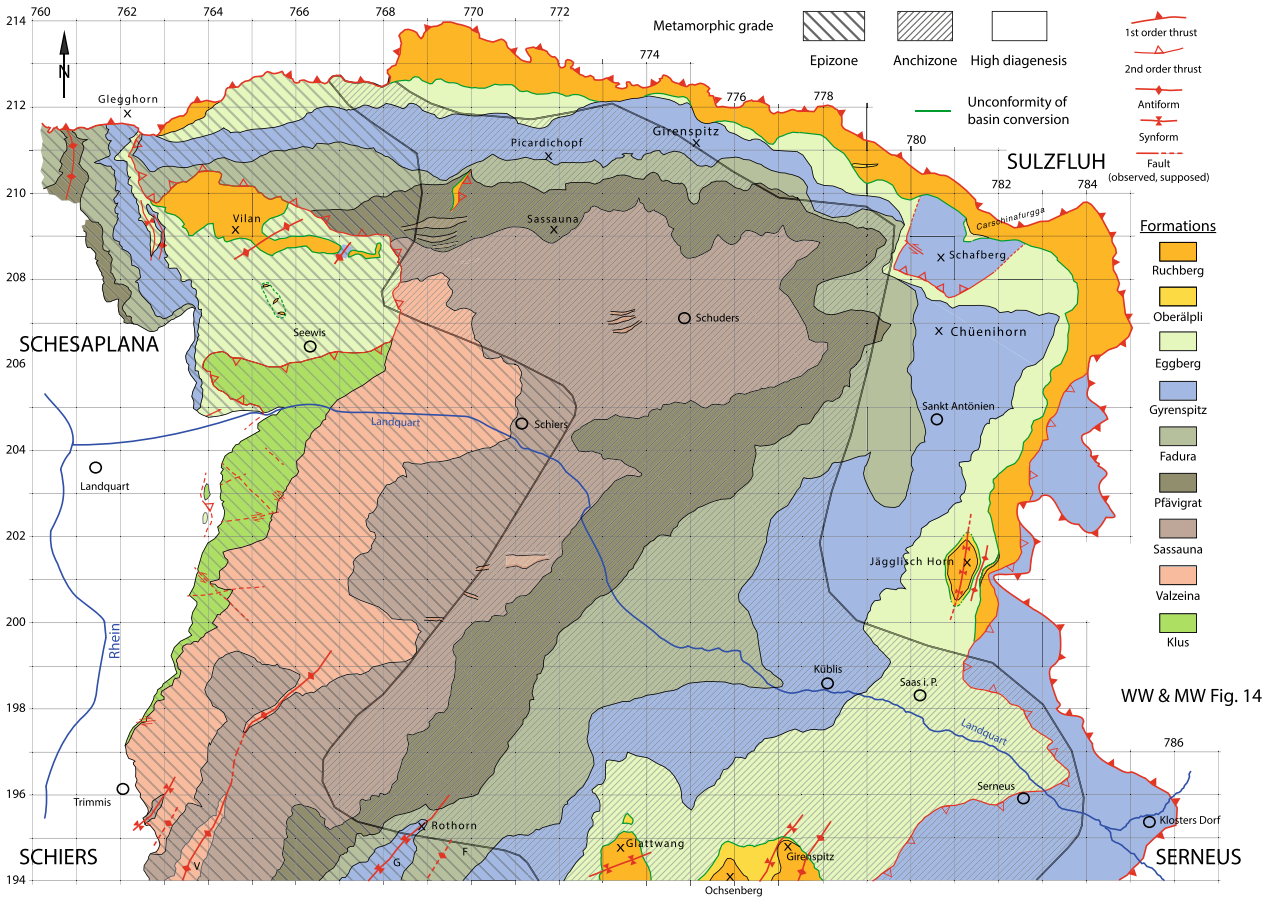

Fig. 14 Simplified map of metamorphic grade in the northern Prättigau half-window (after Petrova et al., 2002, and references therein). Note that the Palaeogene formations are preserved at medium to higher diagenetic levels

association indicates Zone P3 (ca 64–60 Ma, early-middle Palaeocene) (Serra-Kiel et al. 1998).

3.9 Ruchberg formation

The dominant lithology of the Ruchberg Formation is massive sandstone up to metre thick alternating with thinner sandstones and shales (Fig. 6j, k). In detail, the strata consist of different turbiditic facies. The thick beds are texturally immature (poorly sorted) graded coarse sandstones, which may carry a tractive conglomerate at the base. Thinner beds show complete Bouma sequences or finer intervals thereof. These facies are arranged cyclically with coarsening or fining in the direction of younging (Fig. 6k). On freshly broken surfaces, the sandstones are grey which are weathered to a rusty red and often overgrown with variegated lichens. In another variety of this massive facies, as also noted by Nänny (1948), massive metric grey-blue (yellowish weathered) marls also occur above the graded sandstones. In these facies the sandstones are very rich in detrital white mica.

The Ruchberg Formation was studied early by Arni (1933, 1935) for benthic large *foraminifera*. A re-evaluation of the taxonomy by Giovanni Colleti (University of Milano-Bicocca, 2021) revealed that isolated *foraminifera* (*Orbitolites* and *Siderolites*) were reworked from the Cretaceous (Boudaugher-Fadel, 2018). In addition to *Nummulites planatus, N. subplanatus, N. irregularis* described in Schaub (1981), the presence of *Operculina granulosa* (*Assilina granulosa* in Arni 1935), *N. praelucasi* and *N. spirectypus* in particular confirm the previously determined Ypresian age. In the locality Gross Platte Silvia Spezzaferri (Univ. Fribourg) detected fragments of Acaranids and *Praemurica* cf. *incostans* correlatable with late Palaeocene and younger.

3.10 Special lithologies

At the northern edge of the Prättigau half-window, in similar stratigraphic position as the Ruchberg Formation, a fine-grained sandstone facies occurs. According to its position above the Oberälpli Formation and clear lithological difference, we call it informally distal Ruchberg

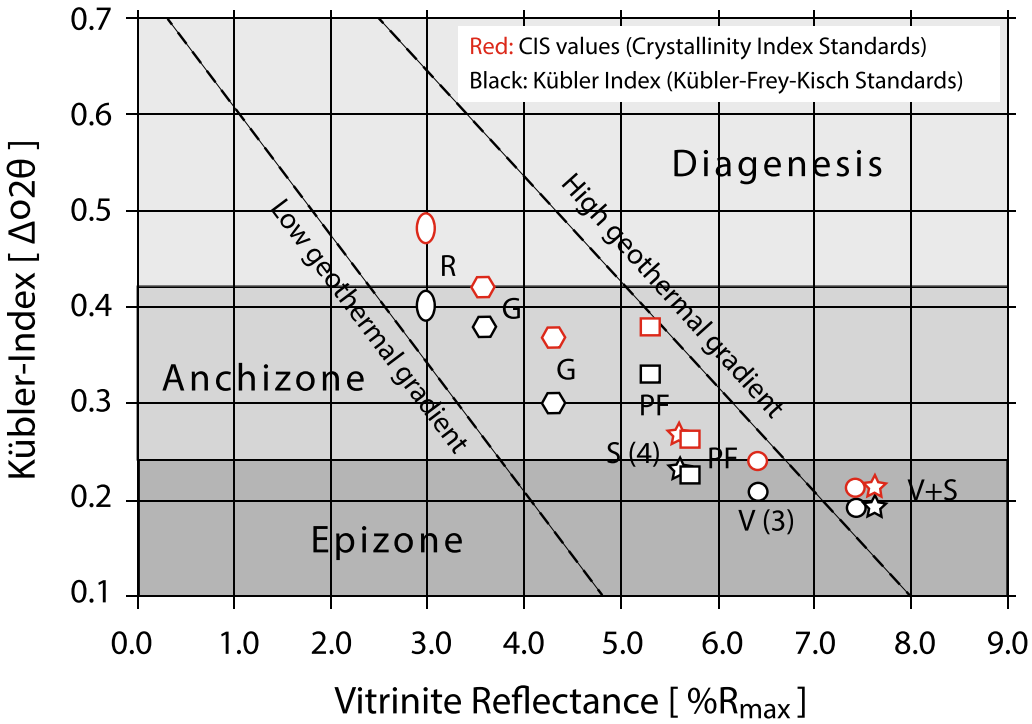

Fig. 15 Diagenesis and metamorphic grade versus vitrinite reflectance of Bündnerschiefer and Flysch in a trace from Vilanspitze to the Plessur river near Chur (Figs. 2, 4). Data from Petrova et al., (2002, black symbols) homologised according to illite crystallinity standards (CIS) from different laboratories by Ferreiro Mählmann and Frey (2012, red symbols). Formations: R, Ruchberg; G, Gyrenspitz; PF, Pfävigrat; S, Sassauna; V, Valzeina. Note that the authors Ferreiro Mählmann and Frey (2012) suggest that the combined use of laboratory standards provides a more accurate picture of the transition from diagenesis to anchizonal metamorphism

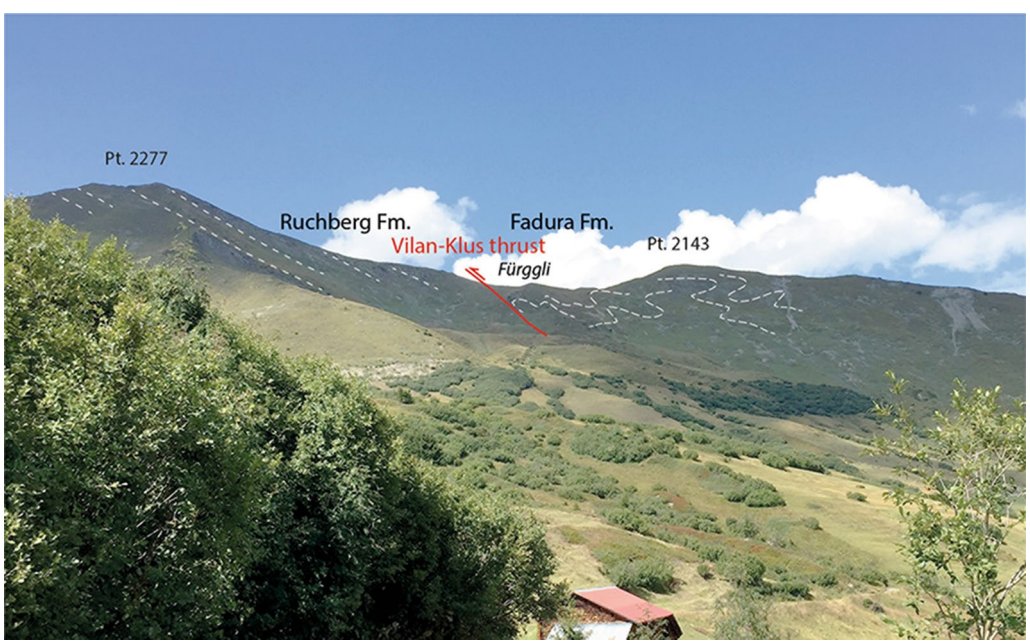

Fig. 16 Panoramic view of the Vilan-Klus thrust at the Fürggli site, NE of Vilanspitze

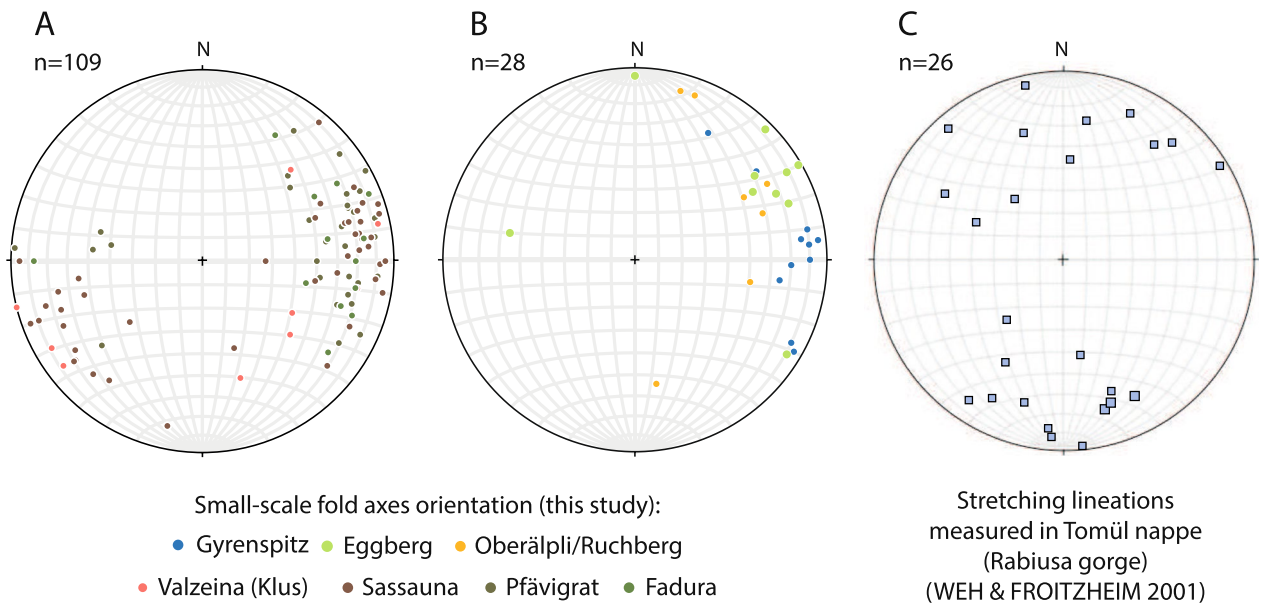

Fig. 17 Stereoplots (lower hemisphere Schmidt projection) of the measured fold axis linears. **A** Measurements in the Valzeina (few Klus), Sassauna, Pfävigrat and Fadura formations; **B** Measurements in the younger formations including the Gyrenspitz to Ruchberg formations; **C** Stretching lineations in the Bündnerschiefer of the Tomül Bündnerschiefer in the Rabiusa Gorge near Passugg (Weh and Froitzheim, 2001)

Formation (Fig. 5). It consists of mica-rich brownish-grey siltstones and marls laminated on a scale of mm-cm and fine cm-thick sandstones with partly undulating surfaces (Fig. 6l). On the Sulzfluh sheet this lithology is well exposed in the localities of Carschinahütte (Swiss Grid Coord.. 2781.530/1209.070) and on the southwestern slope of the Chläsi hummock (Swiss Grid Coord. 2778.860/1210.524). On the Schesaplana sheet, it directly covers the Eggberg Formation in small outcrops along forest roads in the Bawald region northwest of Seewis: Pligugg (Swiss Grid Coord. 2765.562/1207.800) and Bawald (Swiss Grid Coord. 2765.428/1207.567). Such a laminated sandstone in the Pligugg locality revealed reworked Cretaceous planctonic *foraminifera*, a specimen *Globanomalina* cf. *archeaocompressa* and *Morozovella subbotinae* from range zone P5-P7, i.d., the transition to the Eocene (pers. comm. Silvia Spezzeferri 2021).

Similarly, the deformed Eggberg Formation is covered by a small-scale alternation of grey, reddish and yellow weathered marls and clays (Fig. 6m). We informally call this lithology variegated marlstones. This occurrence, very remarkable for the region, was found along the inner bank of the forest road near Alpe Gilieila. (Swiss Grid Coord. 2765.050/1207.826) northwest of Seewis (Fig. 4). Marl samples were analysed for nannoplankton (written comm., Eric de Kaenel, 2018) and revealed a wide range of Late Cretaceous forms. The youngest species identified was *Micula swatsica*, which is assigned an age of Late Campanian to Maastrichtian. (http://www.mikrotax.org/Nannotax3/ntax-forum.php). This hitherto unknown non-metamorphic lithology raises puzzles about its stratigraphic position and the conditions of formation in the Prättigau series (Fig. 5). The simple process of reworking during the Palaeocene seems rather unlikely, as this sediment shows a clean marly composition. A tentative suggestion is discussed in more detail below.

4 Arguing for the presence of an unconformity between the Cretaceous and Palaeogene formations

4.1 Formation boundary situations

In the Prättigau, the Ruchberg Formation and its distal equivalents overlie older formations in various ways (Fig. 8). The complete Palaeogene succession is recognised where the Oberälpli Formation can be observed in the areas of Ochsenberg, Chläsi and Jägglisch Horn (Fig. 4), and Sunnetäli south of Ochsenberg (Fig. 9). The transition is more gradual with the increase in sandstone layers within black shales over a thickness of several metres in the steep terrain on the northern ridge of the Ochsenberg. In the Vilan (Fig. 4), however, the massive Ruchberg rests above the folded Eggberg. This situation is exposed in detail along the forest road in the Wurzaneinawald locality (Swiss Grid Coord. 2766.635/1208.620) (Fig. 10). There the shallowly northward dipping Ruchberg Formation unconformably overlies the folded, foliated and epizonal-metamorphosed Eggberg Formation.

South of the Carschinafurgga, the Oberälpli Formation and distal Ruchberg Formation overlie the northward

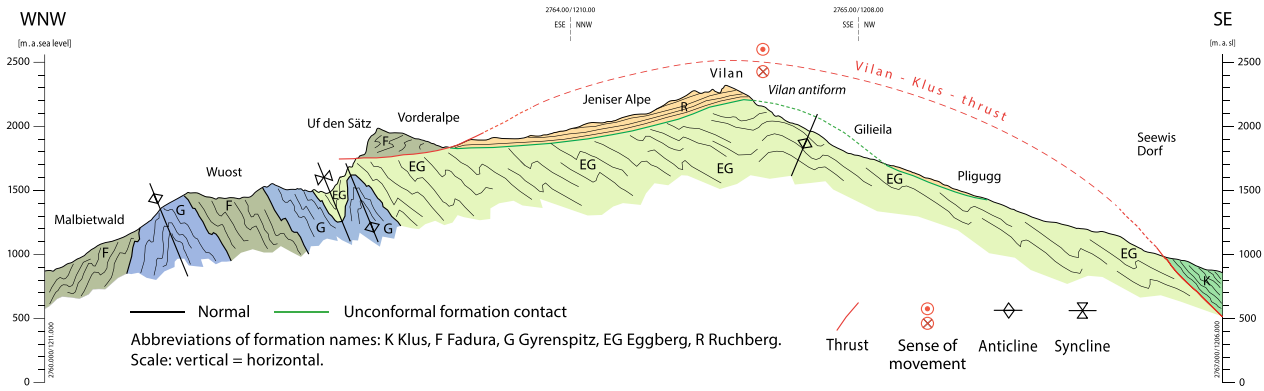

Fig. 18 Geological profile through the north-western part of the study area on the Schesaplana sheet (see Fig. 4). The sketch shows the Vilan-Klus-thrust bringing a stack of Bündnerschiefer series towards the observer over the Ruchberg Formation, which is in unconformable sedimentary contact with the Eggberg Formation. Later doming of the Prättigau caused the upward bulging of the thrust plane. Note that the distal Ruchberg Formation is present at the Pligugg locality and the variegated marlstones were mapped at Alpe Gilieila

dipping Gyrenspitz Formation (Fig. 11). In the Gross Platte area, a wedge of massive beds of a mica-rich Ruchberg Formation variety, about 80 m thick, is observed on folded Pfävigrat Formation, and is in turn overthrust by the latter one (Figs. 6j, 12). The remnant cover of the Eggberg Formation by the distal Ruchberg Formation and the above-mentioned variegated marls (Figs. 4, 6m, 9) can be seen in the wider area of the Bawald (Pligugg-Galileia), north-west of Seewis (Fig. 4).

4.2 Provenance of detrital clasts

It is common to observe changes in lithology and terrigenous source across sedimentary unconformities. This is also evident from our thin section analyses, as the Ruchberg Formation contains higher levels of rock fragments, quartz and plagioclase than the Cretaceous formations (see also Thum and Nabholz, 1972).

Further evidence came from U–Pb age distributions of detrital zircons in selected Prättigau formations (Beltràn-Triviño et al., 2013). We have extended and completed such data for the present work. However, we were unable to date sufficient zircons from the Gyrenspitz Formation due to their rarity and the predominance of sedimentary lithoclasts. It is noteworthy that the various micritic limestone clasts observed in the Gyrenspitz Formation (see above) show a strong affinity with lithologies preserved in the Sub-Briançonnais unit of the Middle Penninic. Therefore, a detrital input from this southern adjacent Middle Penninic ridge can be assumed.

As shown in Fig. 13, the Cretaceous formations on the right column contain, with few exceptions, a limited age range of Palaeozoic zircons. The Palaeogene formation results are arranged in Fig. 13 (left column) roughly according to their assumed stratigraphic position, from bottom to top. Two features are observed: (1) in comparison with the Bündnerschiefer sandstones (right column) the Flysch detrital zircons become increasingly variable and older in their ages, extending back into the Meso-Palaeoproterozoic; and (2) the Flysch sandstones consistently contain Triassic detrital zircons. It seems therefore, during the Palaeogene flysch stage a change in the clastic supply of the basin took place which was completed by the Early Eocene (Ypresian) at the latest.

4.3 Metamorphism

The profile of the North Penninic Bündnerschiefer and Flysch of the Tomül nappe in the Prättigau shows that the metamorphic overprint increases stratigraphically downwards and in a south-westerly direction (Figs. 4, 14). The compilation was done using publications by Thum and Nabholz (1972), Steinmann (1994), Frey et al. (1999), Frey and Ferreiro Mählmann (1999), Ferreiro Mählmann et al. (2002), Petrova et al. (2002), Wiederkehr et al. (2008), Wiederkehr et al. (2009), Ferreiro Mählmann and Frey (2012). The metamorphic pattern has been documented by a variety of methods including thin section and mineral paragenesis analysis, measurements of illite crystallinity and degree of carbonation, and vitrinite reflectance. The Ruchberg and Oberälpli formations on the northern and eastern margins of the Prättigau half-window are preserved in the higher diagenetic stage which is also evident from field observations and from our thin section studies (Figs. 14, 15). This applies in particular to all other occurrences of the Oberälpli and Ruchberg formations above the higher metamorphic zones, such as in the Vilan, Glattwang and Ochsenberg-Girenspitz mountains (Fig. 14). Consequently, also the epizonal (greenshist facies) metamorphism present in the Bündnerschiefer (Fadura Formation), which overthrusts the Ruchberg

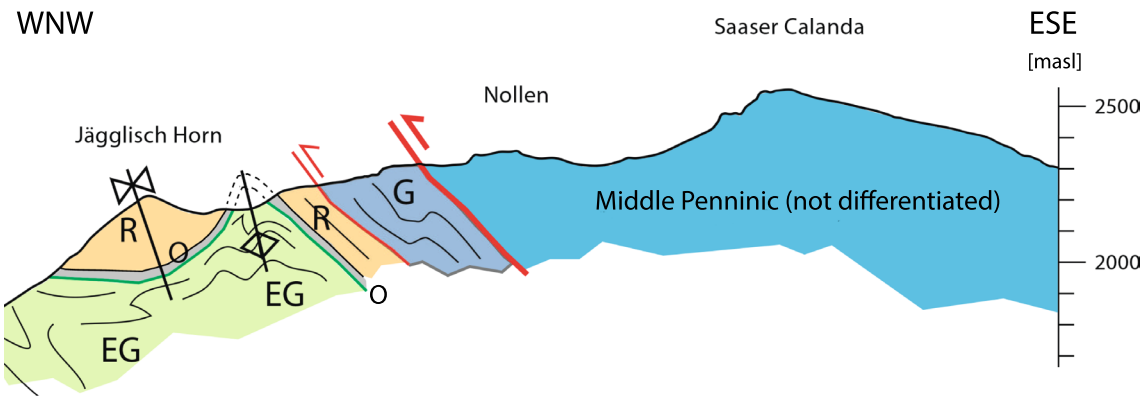

Fig. 19 Geological profile through the eastern margin of the Prättigau half-window in the Jägglisch Horn area (for location see Figs. 4). Symbols and abbreviations as in Fig. 11 and 20

Formation in the Vilan area (locality Fürggli, and part of our Vilan-Klus thrust, Fig. 4, 16), was tectonically transported. In summary, the Palaeogene flysch formations are preserved in a highly diagenetic stage and overly folded anchi- and epizonal Cretaceous formations.

Towards SW up to the Chur and Plessur area, the regional pattern of metamorphic grade suggests the presence of a higher geothermal gradient during metamorphism of the Tomül nappe (Fig. 15, Ferrero Mählmann and Frey 2012). South of Chur, undifferentiable sediment formations of the Tomül nappe series were metamorphosed in low blue schist facies (Bousquet et al., 2002, Wiederkehr et al., 2008), which is among others indicated by the occurrence of Fe–Mg carpholite. Wiederkehr et al., (2008, 2009) determined an age of maximum metamorphism of 43–40 Ma ($^{40}Ar/^{39}Ar$) at ca. 350–400 °C and 1.2–1.4 GPa pressure at ca. 50 km depth, based on different muscovite generations associated with the carpholite.

5 Tectonic structures

The frame of the Prättigau half-window (Fig. 2) consists, from base to top, of limestone sequences of Middle Penninic units (Fig. 3b), the Arosa Zone with partly ophiolitic melanges and scales of South Pennine and Lower Austroalpine age (e.g. Lüdin, 1987; Winkler, 1988; Signer et al., 2018), and crystalline and sedimentary nappes of the Upper Austroalpine. At the bottom of the Prättigau half-window, the basal North Penninic thrust overlies Lower and Upper Helvetic units (Pfiffner, 2014).

The formation boundaries are oriented SW to NE in the southern part of the Prättigau half-window (see Fig. 4), while in the north they run E–W parallel to the major thrust faults in the hanging wall. On the Schesaplana and Sulzfluh sheets, the formation boundaries turn westward and run parallel to the main northern margin to the Middle Penninic units (a main or 1st order overthrust; Fig. 4). To the east, a secondary or 2nd order overthrust runs parallel to the half-window boundary. This overthrust places the Gyrenspitz Formation on top of the Ruchberg and Eggberg formations. This situation was already recognized by Nänny (1948). However, Weh and Froitzheim (2001) did not distinguish this thrust fault, because they did not consider the lithostratigraphic subdivision of the Prättigau series for their structural analyses. East of Landquart, an important thrust fault puts the Klus, Valzeina, Sassauna, Pfävigrat and Fadura formations *en bloc* onto the Eggberg and Ruchberg formations (Fig. 18). Because of its much larger dimensions, we call it the Vilan-Klus overthrust. Weh and Froitzhein (2001) recognised the northern part of the overthrust and called it the Vilan overthrust. As a detail, at the Fürggli locality, the folded Fadura Formation overthrust onto contiguous sandstone beds of the Ruchberg Formation dipping to the northeast (Fig. 16). Of further interest are the stratigraphic cutoff points ("triple points") which occur along the Klus-Vilan thrust which became visible by mapping the lithologic boundaries. More specifically, the thrust cuts up-section through the formation boundaries towards the NW.

A further major thrust fault, the Schafberg thrust, is located in the NE corner of the Prättigau half-window (Fig. 4, 11). It dips to the NNE and puts the Gyrenspitz Formation onto the Eggberg Formation. Similarly, the unconformity between the Gyrenspitz and Oberälpli formations at Carschinafurgga also dips to the NNE (Fig. 11).

Prominent steep to vertical isoclinal fold structures run in approximately S-SW to E-NE direction. We have labelled them as Rohnentobel, Salginatobel and Mühlieggtobel antiforms in Fig. 4. Beautifully exposed M-folds in the Sassauna Formation in the Schraubach between Schiers and Schuders (Fig. 4) are similarly

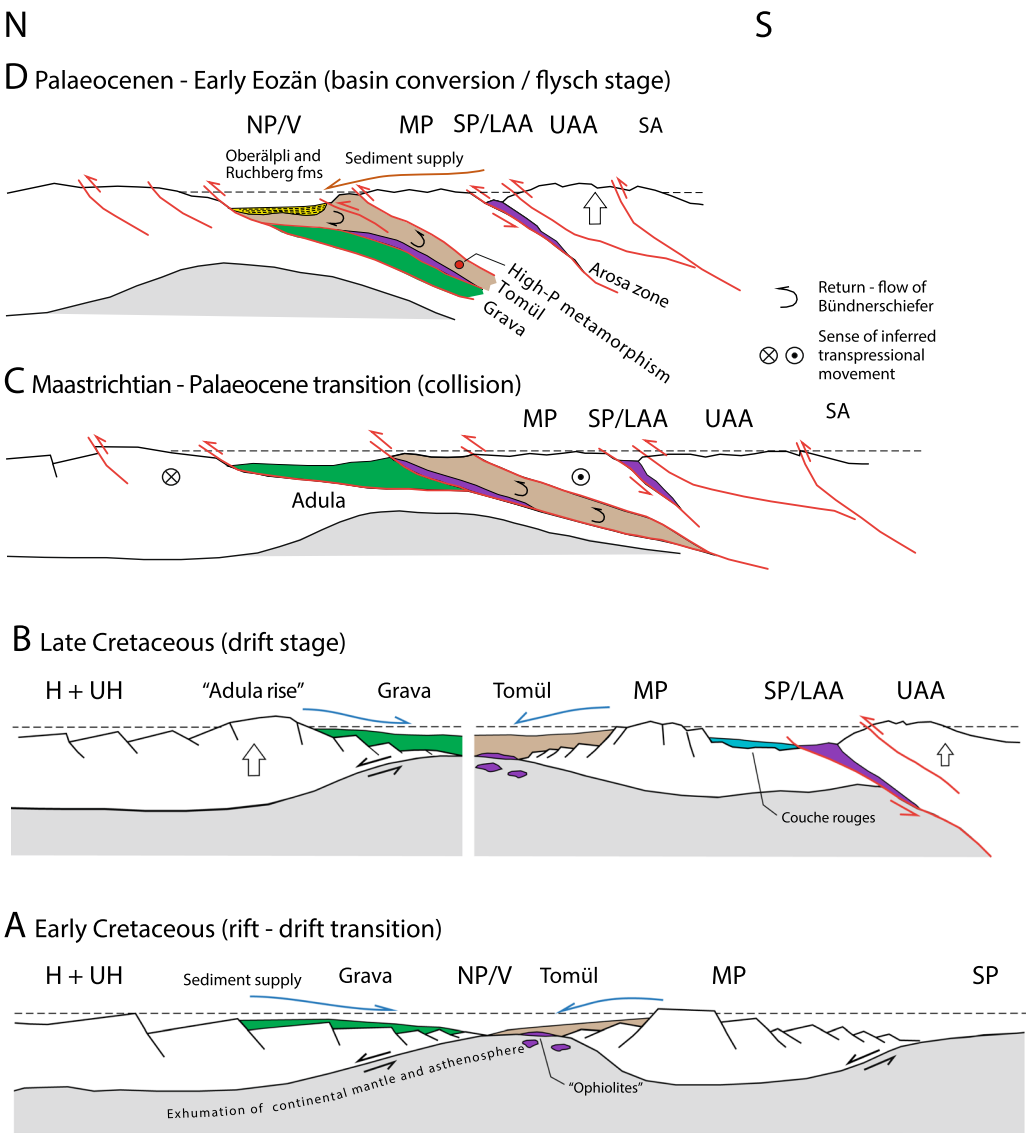

Fig. 20 Schematic palinspastic profiles of the development of Bündnerschiefer and Flysch in the North Penninic/Valais section of the Prättigau half-window (not to scale). Drift stage according to Steinmann (1994). The flysch stage follows the basin conversion and is still active in the Tomül nappe depositional area. The Grava nappe area was probably tectonically buried such that no flysch could be deposited there. Unit abbreviations: AA, Austroalpine; H, Helvetic; NP/V, North Penninic/Valais; MP, Middle Penninic; SP, South Penninic; UH, Ultrahelvetic; LOA, Lower Australpine

orientated. If outcrop conditions were better, this type of structure would be observed much more frequently. The majority of the folds attributed by Weh and Froitzheim (2001) to their deformation phases D2 and D3 show similar orientations, fold axes trending WSW-ENE and plunging to the WSW (see Fig. 4). Viewed at large scale, the Bündnerschiefer and Flysch succession form a large SW–NE trending antiform in the Prättigau half-window. This was most likely caused by late uplift of the Aar massif (Pfiffner, 2014, Herwegh et al., 2017).

A detailed structural analysis of the series was beyond the scope of this study. However, we attempt to reconstruct the history of tectonic deformation of the series based on a large number of measurements of small-scale fold axes and mapping of large-scale tectonic structures. Our measurements of the small-scale fold axes and fold hinges, shown in the stereogram in Fig. 17a, plunge to the E-NE or W-SW at variable but mostly small angles (≤ 40°). The fold axes in the younger formations (Gyrenspitz, Eggberg and Oberälpli/Ruchberg) mostly dip at small angles to the E and NE (Fig. 17b), probably as a

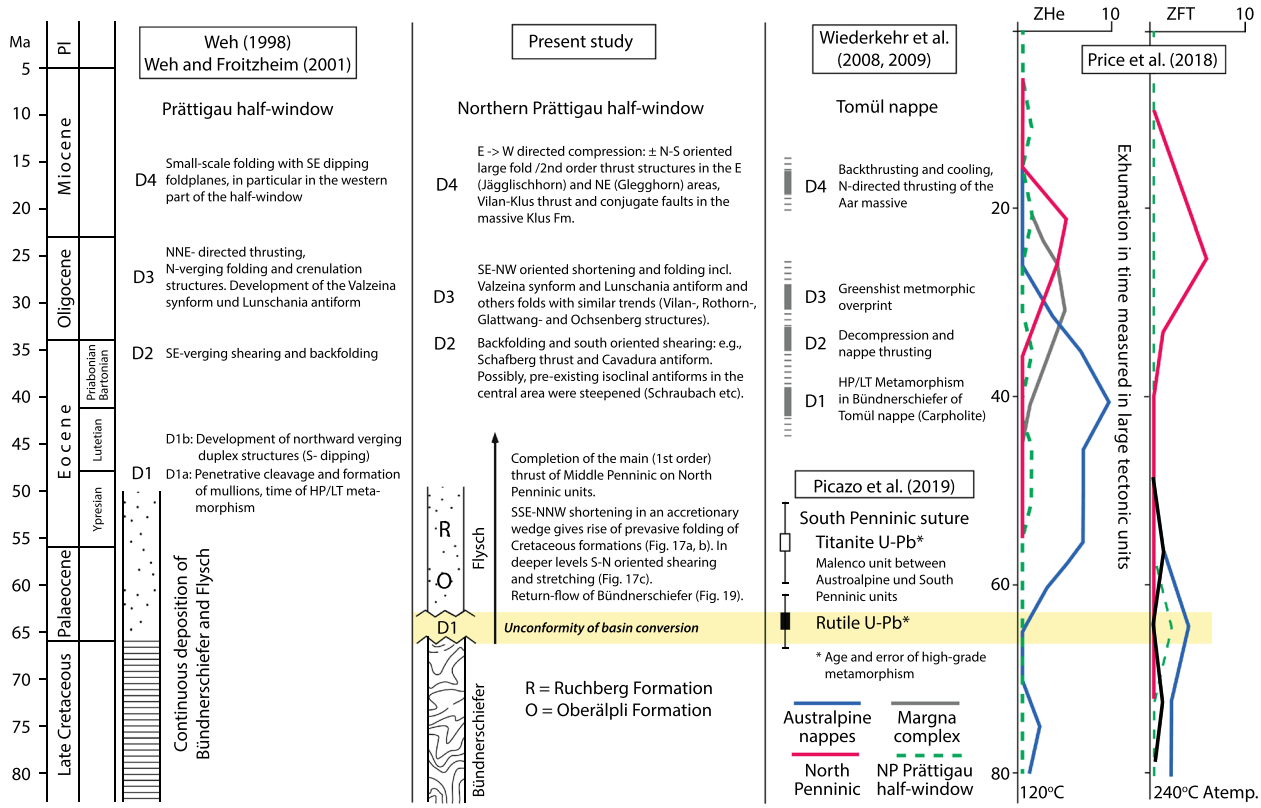

Fig. 21 Comparison of structural and metamorphic data for reconstructing the Cenozoic basin and tectonic deformation history of the North Penninic Tomül nappe in the Prättigau half-window. Exhumation/cooling rates in the relevant tectonic units according to Price et al. (2018): ZHe = (U-Th)/He; ZTF = zircon fission traces (Atemp. = approximate annealing temperatures). See text for further details

result of later tectonic tilting to the east of the half-window, i.e. by the formation of the antiform mentioned above. Similar orientations and plunges with corresponding poles of axial plane schistosity were reported in the inner Tomül nappe SW of Chur by Steinmann (1994). The stretching lineations measured by Weh and Froitzheim (2001) in undifferentiated Bündnerschiefer of the Tomül nappe in the Rabiusa Gorge near the village of Passugg (Fig. 17c) are at an angle of ± 90° to the fold axes.

The dominant tectonic structure is the small-scale folding of the Bündnerschiefer, which is attributed to a first deformation phase, D1. These folds were subsequently redeformed by D2 and D3. D2 involved S-directed shearing and backfolding, while D3 produced the large-scale Lunschania antiform and the Valzeina synform in the south-western part of the study area (Fig. 4, Weh and Froitzheim 2001). Deformation phase D3 is manifested by a crenulation cleavage as observed in a displaced block of the Pfävigrat Formation (Fig. 10) and by an in-situ measured SW dipping crenulation cleavage in the Sassauna Formation. More difficult to understand is the eastward rotation of the axis of the Lunschania antiform, which connects to the Mühlieggtobel antiform as interpreted by Weh and Froitzheim (2001) (see Fig. 4). We suggest that the Mühlieggtobel antiform formed at different time.

Only large-scale deformation structures are present in the Palaeogene flysch sediments (Fig. 10). SSW-NNE oriented folds dominate the southern margin of the study area from the Rhine valley to the Ochsenberg/Gyrenspitz area in the east, deforming the Cretaceous Bündnerschiefer and the Palaeogene flysch (see Fig. 4). In the Bündnerschiefer a large scale syncline, the Rothorn syncline runs parallel to the Lunschania antiform and the Valzeina synform.

Other major tectonic structures are oriented N-S. They include the narrow synform in the area of the Jägglisch Horn which formed due to the thrust fault putting Gyrenspitz over Ruchberg Formation (Fig. 19). Additional narrow synforms trending N–S occur at the NW tip of the study area (south of Glegghorn; see Fig. 4). Together with the Vilan-Klus overthrust (Fig. 18), the conjugate fracture systems in the Klus Formation and the overthrust of the Ruchberg Formation by the Pfävigrat Formation near

Gross Platte (Fig. 4 for location and Fig. 9) indicate an east–west tectonic narrowing.

6 Discussion and interpretations

6.1 Comparisons of the Prättigau North Penninic with units in other areas

A recent study by Rauch (2014 and references therein) of the North Penninic in the Lower Engadine window describes at Piz Mundin a basal sequence of radiolarites and red schists overlying pillow lava basalts. These in turn are overlain by: (1) limestones and marls interbedded with fine breccias, (2) black shales and quartz sandstones, and (3) calcareous sandstones alternating with black shales.

In the area of the Petit Saint Bernard Pass in Italy we find another sequence typical of the North Penninic or Valais zone. This is where the so-called Valais trilogy was originally coined (see e.g. Loprieno et al., 2011; Beltrando et al., 2012 for an overview and references). Generally, between extensional Palaeozoic-Mesozoic allochthonous blocks, the sequence shows exhumed mantle (serpentinites) and mafic intrusions. These are covered by the trilogy represented first by siliceous limestones and breccias (Aroley beds), then by dark shales with quartz sandstones (Marmontain beds), and finally by a thick turbiditic sequence of calcareous sandstones and shales (St Christophe beds). A recent study by De Broucker et al. (2021) attributes to the Late Cretaceous St. Christophe unit the status of a flysch sequence. These researchers propose the formation of an accretionary wedge in the Valais area as early as the Early Cretaceous. This wedge contained tectonic mélanges and would have been sealed by the triology.

However, according to Loprieno et al. (2011), a Jurassic to Early Cretaceous rifting occurred in the Valais palaeogeographical region of the Savoy Alps and involved the southern part of the European plate margin. The Valais trilogy should have discordantly overlapped external European and internal ophiolitic series. Loprieno et al. (2011) explain the hP/lT metamorphism that affected the units by the collision of the Middle Penninic (Briançonnais) with the distal European plate margin (Dauphinois) during the Eocene.

These two well-studied examples show an affinity with the the older units of the Tomül and Grava nappe cover rocks in the Rheinwald area described by Steinmann (1994). In the Tomül nappe metabasalts are followed by sandy and dark limestones with black shale intercalations (Bärenhorn Formation), dark shales partly rich in organic carbon with sandstones (Nollaton Formation) and medium- to coarse-bedded clayey limestones (Nollakalk Formation). In the Grava nappe the uppermost stratigraphic unit is the Carnusa Formation, which consists of turbiditic sandstones and shales of unknown age. By comparison, in the Tomül nappe of the Prättigau, the Cretaceous series appears to be more distinct (or complete?) and unconformably capped by Palaeogene flysch deposits.

The extension model of Steinmann (1994) with exhumed asthenosphere combined with low magmatic activity (Manatschal and Müntener, 2008) seems to explain rather well the early palaeotectonic history of the North Penninic in these palaeogeographical realm (Fig. 1). In the Prättigau area, however, the Upper Cretaceous series can be clearly divided into individual turbiditic formations, and the Palaeogene formations unconformably overlie the older ones. It is also worth noting that Palaeogene sedimentary sequences have not yet been identified elsewhere in North Penninic or Valais units.

6.2 Basin evolution

The lithostratigraphic subdivision of the Cretaceous and Palaeogene series by Nänny (1948) proved its worth, although experience is needed to grasp the lithological nuances in isolated outcrops. Major modifications were made to his map in the Vilan area, where the geographical extent of the Ruchberg Formation had to be greatly reduced An earlier valuable structural analysis was provided by Weh (1998) and Weh and Froitzheim (2001). However, they considered the entire Bündnerschiefer and Flysch sequence to be a single unit, and accordingly, tectonic deformation should have started only after the deposition of the Ruchberg Formation in the Early Eocene.

We think the key point is our finding that the Palaeogene formations overlie the Cretaceous unconformably. This means that an earlier deformation affected the Cretaceous Bündnerschiefer series series. If this unconformity is accepted as described above, we can re-evaluate the sedimentary history and tectonic evolution from a different point of view.

There is general agreement that the North Penninic Bündnerschiefer were formed during the Cretaceous extensional phase along the European margin by rifting of the Middle Penninic continental margin or the Briançonnais block. (Fig. 20, e.g. Schmid et al., 1990, 2004; Schreuers, 1993; Steinmann, 1994; Stampfli et al., 2002; Schmid et al., 2004). According to this model, sediments of the Grava and Tomül nappes should have been deposited on both sides of the rift (Fig. 20a). In contrast to the Grava realm, in the Tomül realm exhumation of the continental mantle and asthenosphere resulted in Late Jurassic-Early Cretaceous basaltic extrusions at the base of the Early Cretaceous Bärenhorn Formation ("Tomüldecke-Grüngesteinszug", Steinmann; 1994; Wyss and Wiederkehr; 2017), derived from depleted MORB-type mantle (Steinmann and Stille; 1999).

During the extensional phase, the lithostratigraphic characteristics of the mainly turbiditic formations were determined by the temporally variable qualitative and quantitative influx of terrestrial siliciclastics and the basin-internal carbonate/organic production. For the Grava realm, exhumation of the asthenosphere may have produced the hypothetical Adula Rise as an important clastic source (Fig. 20b), as has long been postulated by Nänny (1948) and Trümpy (1980). In the southern margin of the basin, the later Tomül nappe series developed with many similarities to the Grava basin as neatly correlated by Steinmann (1994, e. g., his Fig. 17). For earlier researchers (e.g., Jäckli, 1941; Nänny, 1948; Trümpy, 1980; Bundesamt für Landestopographie 2005) following the traditional geosynclinal model the start of flysch deposition in the Tomül palaeogeographic realm was correlated with the onset of coarser clastic deposits such as the Hauptkonglomerat (e.g., Jäckli 1941) in the Stätzerhorn Group (Burla 1997). The age of these coarse clastics would have more or less coincided with the Pfävigrat Formation in the Prättigau. According to our observations in the Prättigau series this view needs to be revised: mapping revealed a large-scale unconformity which shows more complicated bedding relationships between the Cretaceous and Palaeogene formations (e.g. Fig. 9).

In our perception, at the transition from Cretaceous to Palaeogene the basin conversion took place due to the onset of subduction in the entire North Penninic realm (Fig. 20c). As a result, the Cretaceous series of the Grava and Tomül basins have been overthrusted by the Middle Penninic units and have been deformed in an accretionary wedge. At the same time, the Grava sedimentary domain was probably eliminated as a depositional site through overthrusting. In the remaining Tomül basin, flysch sedimentation started, as also manifested by the qualitatively changing supply of the basin from the emerging Austroalpine units (Fig. 20c). Return-flow from the subduction channel transported deformed Bündnerschiefer into the reconfigured trench basin, resulting in a variable stratigraphic basement for the flysch deposits. The irregular thickness of the Oberälpli Formation, or its total absence (already observed by Nänny, 1948), suggests that it initially deposited in local depressions during basin conversion, as a result of restructuring of the basin floor morphology. The special lithology of coloured marls, which are probably in contact with the folded Eggberg Formation, could indicate starved sedimentation during the conversion of the basin. Subsequently, the Ruchberg Formation prograded from the south basinwide with a northward fining/thinning trend (Fig. 20d).

An increasing influx of erosional material from the developing Australpine nappe edifice, bypassing parts of the Middle Penninic units, can be inferred from the modified U–Pb age patterns of detrital zircons. Finally, after decades of unsuccessful searches for Palaeogene flysch formations in the Grava and internal Tomül nappe, e.g., the Stätzerhorn Group, one may have to conclude that they do not exist at all, because the sedimentation areas probably have been tectonically eliminated by the processes described.

6.3 Timing of tectonic deformation

The Bündnerschiefer and Flysch of the Prättigau have been structurally studied by Weh (1998) and Weh and Frotzheim (2001), taking into account the assumed contemporaneous deformation in the overlying Middle Penninic Falknis nappe in the Gürgaletsch area (Fig. 2). The authors interpreted the onset of the deformation history stratigraphically after the deposition of the youngest formation (Ruchberg), i.e. 50–48 Ma (late Ypresian, Fig. 21).

However, the presence of unconformable contacts of the Oberälpli or Ruchberg formations with the folded Eggberg, Gyrenspitz and Pfävigrat formations (Fig. 9) argues that the Bündnerschiefer were already deformed at the end of the Cretaceous and that these older formations were tectonically transported back to the basin floor by return-flow in a subduction channel (e.g., Moulas et al., 2021; Kotowski et al., 2022). These authors presented a petrological and metamorphic geochronological study on the island of Syros in the Greek Cyclades to reconstruct the Eocene–Oligocene return-flow of subducted and underplated nappe units over the period of ~50–20 Ma.

In the North Penninic/Valais realm, this process took place as a result of the basin series being transformed into an accretionary wedge. This was achieved by compression and folding from the south to the north. We postulate that this deformation resembles in style to the phase D1a and D1b introduced by Weh (1998) and Weh and Froitzheim (2001), which according to these authors formed riffle folding ("mullions") and schistosity in the deeper levels of the growing Bündnerschiefer accretionary wedge (Weh and Froitzheim, 2001, p. 245). According to our mapped bedding relationships, an initial generally south-to-north compressional movement in the accretionary wedge caused penetrative folding in the Cretaceous formations (Fig. 21). This process produced the small-scale folds with shallow WSW and NNE plunges (Fig. 17a, b). At deeper levels of the accretionary wedge, shearing and stretching occurred at this time, as proposed by Weh and Froitzheim (2001, see Fig. 17c. We believe that the earliest deformation in the Prättigau nappe occurred during the D1 phase. Later deformation consisted of large-scale folding and fracturing over hundreds of metres and kilometres.

Weh and Froitzheim (2001) were reluctant to separate D1a and D1b phases because of a lack of arguments as to whether they were temporally or genetically distinct. They refer to known processes in accretionary wedges, where folding at higher levels occurs simultaneously with accretion at depth. In contrast, accretion and sedimentation occur simultaneously in subduction margins, and we would combine the two processes under the deformation period D1 (Fig. 21).

Nevertheless, the unconformity and flysch deposition occurred coevally with dated high-grade metamorphism in the Malenco unit between other Austroalpine and South Penninic units (Fig. 21) as recognised by Picazo et al. (2019). Zircon (U-Th)/He and zircon fission-track thermochronological results (Price et al., 2018) from the tectonic units involved show, in particular, increased exhumation rates from the Palaeocene to the Eocene in the Austroalpine allochthons. This is corroborated by the shift to Austroalpine sediment sources we observe in the detrital U–Pb age patterns. According to the age data of the carpholite-bearing rocks (43–40 Ma, Wiederkehr et al., 2009), the hT/lP metamorphism in the Tomül nappe should have occurred during Middle to Late Eocene (Fig. 18). This age, however, is much younger than the Palaeogene unconformity and basin conversion (Fig. 18). In our view the this hP/lT metamorphism occurred with the thrusting of Middle Penninic units over the North Penninic units.

The mapped structures at the hundred metre and kilometre scale are approximately parallel to, and tentatively correlate with, the SE-trending shear and refolding of phase D2 of Weh and Froitzheim (2001). Although more SSW oriented, the Schafberg thrust and the south-verging Cavadura anticline should represent this back-thrusting event (Figs. 4, 11). It is also possible that the common SSW–NNE trending antiforms (e.g. Mühlieggtobel, Schraubach, Salginatobel and Rohnentobel) have been rotated to an almost vertical orientation by the backward thrust of the originally recumbant geometry.

We agree with Steinmann (1994) and Weh and Froitzheim (2001) that phase D3 overprints the Tomül and Grava nappes. Accordingly, WNW-ESE oriented compression formed the Valzeina synform and the Lunschania antiform and crenulation cleavage described above. The Vilan, Rothorn, Glattwang and Ochsenberg folds may pertain to D3, given their orientation (Fig. 4). The D2 and D3 phases match the decompression and greenschist facies overprinting phases identified by Wiederkehr et al. (2009) in the Tomül nappe.

We believe that there was another large deformation, which we label D4. First, the steep folding of the Bündnerschiefer with N–S striking fold axis planes in the north-western corner of the window (south of the Glegghorn). Then, the large, bowed Vilan-Klus thrust (Figs. 4, 20), which is well exposed in the Fürggli locality (Fig. 16) pushes westwards the Bündnerschiefer formations *en block* over the Eggberg and Ruchberg formations. In the Gross Platte area (Fig. 12), a wedge of the Ruchberg Formation may be overthrusted westward by the encasing Pfävigrat Formation. Finally, along the eastern edge of the Prättigau Window, the Gyrenspitz Formation overthrusts the Ruchberg Formation to the west, causing folding of the Paleogene formations in front (see Fig. 21).

This late tectonic scenario has to be placed in the larger context of the present tectonic situation. Since the Cretaceous-Paleogene transition, the collision between the European margin and the Adriatic indenter led to transpression in the eastern, central and western Alps, respectively (e.g. Ratschbacher et al., 1991; Steck et al., 2015; Ceccato and Pennacchioni, 2018). During this process, especially from ≈ 20–17 Ma, increased convergence and European slab breakup occurred, accompanied by westward transpressional escape deformation in the western and central Alps (Schmid et al., 2013; Handy et al., 2015; Bertrand and Sue, 2017; Herwegh et al., 2017).

6.4 From subduction to metamorphism

The reconstruction of the tectonic-sedimentary evolution requires the consideration of different aspects such as (1) the chronology of events before and after the end of sedimentation (Oberälpli and Ruchberg formations), (2) the correlation with the metamorphic evolution in the Tomül and Grava cover series and (3) the knowledge of geodynamic parameters such as subduction rate, subduction velocity of the lower plate and subduction angle.

It is extremely important to realise that the time of a dated metamorphism (highest grade) in a rock body should not be equated with the beginning of the process that led to this metamorphism (e.g., Pfiffner et al., 2000). Especially in subduction zones, several million years may elapse before especially the temperature conditions are reached. From this point of view, the basin conversion with the onset of subduction should have started much earlier than the high-pressure metamorphism in the Tomül nappe (Winkler and Wiederkehr, 2019).

With regard to the latter geodynamic parameters, few field examples or computational models exist for the Alps in general and for the present situation (e.g., Pfiffner et al., 2000; McCarthy et al., 2020). Subduction rates of 1–2 cm/year were determined from paleogeographic reconstructions (e.g., Schmid et al., 1996; Pfiffner et al., 2000) are a common approximation. The current subduction rate between Europe and the Adriatic indenter, in the Eastern Alps, is thought to be in the order of 2 cm/year (Kästle et al., 2020). In the Central Alps subduction

appears to be slower in the range of 1 cm/year (Tesauro et al., 2005).

An analogous example, but on a much larger scale, is the collision of the Indian continental plate with the Eurasian continent 55–53 My ago (Kaneko et al., 2003). With a subduction rate of 4.5 cm/year and a subduction angle of 14–19°, the north-dipping Indian plate reaches a depth of 50 km in 3.5 My. Adapted to lower continental subduction rates of ~ 1 cm/yr in the Alps, this depth necessary for high-pressure metamorphism in the Bündnerschiefer (Wiederkehr et al., 2009), could be reached in about 22 My. Data from the Western Alps support this assumption. In the Piedmont-Ligurian area, passive continental margin and oceanic fragments were subducted during the Late Cretaceous. The time between the onset of subduction and prograde high-pressure metamorphism in the Sesia-Dent Blanche and Zermatt-Saas units is estimated to be 22–20 My (McCarthy et al., 2020).

Based on our mapping, we propose that the sequence of Bündnerschiefer was first deformed in an accretionary wedge during basin conversion around the time of the Cretaceous to Palaeocene transition. A new heterogeneous substrate of the basin was created by the return-flow of the Bündnerschiefer units. The Cenozoic flysches came to lie unconformably above this and, in contrast to the Cretaceous Bündnerschiefer, indicate with their composition of sandstones a supply of age-differentiated source areas in the south and west. The flysch was subsequelntly mildly deformed by open folds during phase D3.

According to Pfiffner (1992), the Adriatic microplate underwent dextral transpressive movements relative to the European continental margin during the Cretaceous. For Lihou and Mange-Rajetzky (1996), these movements were responsible for uplifting structural swells that supplied erosional material to neighbouring basins (e.g. Sardona, Niesen, Prättigau, etc.). We suggest that the folding of the Bündnerschiefer at the Cretaceous-Paleogene transition may have been controlled by such transpressive processes (Fig. 21) in the North Penninic Tomül realm.

Our data and thoughts on this suggest that the basin conversion occurred about 20 million years prior to the high-pressure metamorphism dated at 43–40 Ma which affected the same subduction zone (Wiederkehr et al., 2008, 2009). For example, with a hypothetical subduction angle of 30° and a subduction rate of 1 cm/year, subducted parts of the Tomül and Grava covers series could have reached the necessary depth and temperature of 50 km (1.2–1.4 GPa) and 350–400 °C within 20 million years. This period (ca. 65–50 Ma) is also characterized in the overlying blanket stack by pressure-dominated metamorphism in the Malenco unit between Austroalpine and South Penninic units and the above discussed tectonically forced exhumation in Austroalpine ones (Price et al., 2018) (Fig. 18).

7 Conclusions

Re-mapping of the Bündnerschiefer and Flysch in the northern Prättigau half-window has provided new and stimulating aspects of the history and development of the North Penninic/Valais palaeogeography and palaeotectonic evolution in general.

This area preserves in a unique way the transition of sedimentation from a passive to an active continental margin. The Grava and Tomül Bündnerschiefer were deposited during the Cretaceous by extension on top of highly thinned continental crust and exhumed lithospheric mantle, respectively. At the transition from the Cretaceous to the Palaeogene a basin conversion took place. The Bündnerschiefer were deformed for the first time by the incorporation into an accretionary wedge and transported back to the seafloor by return flow. They formed the new and heterogeneous substrate for the Paleocene and Early Eocene flysch units. At the same time, a new flysch basin formed with supply of detritus from exhumed Austroalpine units took place.

Our model of the onset of subduction at the Cretaceous-Paleogene transition fits with the dated hP/lT metamorphism around 43–40 Ma in parts of the deeply buried North Penninic Tomül nappe. Examples of continental collision in different regions and also the estimated subduction rates in the Alpine area of ca 1 cm/year, which compare to subduction rates determined in other orogens, allow sufficient time for these rocks to reach the required pressure and temperature conditions.

Appendix

U–Pb method: The sandstones were crushed by a high-voltage SelFrag device into fragments ≤ 1 mm and sieved to 400–63 µm. Heavy liquid (methylene iodide, 3.32 g/cm^3) and Frantz device magnetic separation followed standard procedures in the mineral-laboratory. Subsequently, zircon grains were picked randomly up to 200 pieces and transferred into qz-beakers; all grains passed through an annealing step with 950 °C and 48 h. After annealing the grains were mounted to epoxy resin blocks and polished. Prior to isotopic analyses, all zircon grains were inspected by cathodoluminescence imaging to check potential inhomogeneities and growth patterns.

Laser ablation ICP-MS U–Pb dating of detrital zircon was performed in a spot mode of 39 µm diameter using an Excimer laser (ArF 193 nm, Resonetics resolution 155) coupled to a Thermo Element XR sector-field ICP-MS in the Institute of Isotope Geochemistry and Petrology (IGP), ETH Zurich (Guillong et al., 2014). A gas-stream was used to transport the ablated material (He, flux rate 1.1 l/s. The laser pulse repetition rate was 5 Hz and the energy density/fluence was ~ 2.0 J/cm^2. Backgrounds

were measured for 30 s and ablation duration was about 40 s. The accuracy and reproducibility of U–Pb zircon analyses were monitored by periodic measurement on external standards (AUSZ7-5, Plesovice, Temora2, 91500, NIST610; Jackson et al., 2004; von Quadt et al., 2014). GJ-1 is used as a primary reference standard for the dating and NIST 610 to calculate the trace element composition using Si (15.2 wt%) as internal standard. Ratios, ages and element concentrations were calculated using IOLITE 3.4 (Petrus and Kamber, 2012). Calculated isotopic ratios and ages were processed with IsoplotR (Vermeesch, 2018) to constrain concordia plots and frequency U–Pb age distribution diagrams.

Acknowledgements
This work was supported by the Swiss Geological Survey in Wabern (swisstopo). We are indebted to Sylvia Spezzaferri, Michèle Caron of the University of Fribourg and Giovanni Coletti of the University of Milano-Bicocca for their advice and help on biostratigraphical issues. Albrecht von Quadt of the ETH Zurich helped us to analyse the U-Pb dating of detrital zircons. Special thanks are due to the reviewers Gianreto Manatschal (Strasbourg), Hugo Ortner (Innsbruck), Roland Wyss (Frauenfeld) and Michael Wiederkehr (swisstopo Wabern) for their constructive suggestions. We would also like to thank O. Adrian Pfiffner, Associate Editor of the Journal, for his numerous suggestions which helped to improve the clarity of the work. With this work we also pay tribute to the former Paul Nänny for his outstanding scientific work in his time, whom the present author knew and appreciated personally.

Author contributions
Not applicable.

Funding
Swiss Geological Service c/o Bundesamt für Landestopographie *swisstopo* Seftigenstrasse 264, CH-3084 Wabern, Switzerland.

Availability of data and materials
Not applicable.

Declarations

Ethics approval and consent to participate
Not applicable.

Consent for publication
Not applicable.

Competing interests
Not applicable.

Received: 4 November 2022 Accepted: 23 January 2024
Published online: 26 March 2024

References

Arni, P. (1933). Foraminiferen des Senons und Untereozäns im Prättigauflysch. Beitr. Geol. Karte der Schweiz, N.F. 65.
Arni, P. (1935). Über die Stratigraphie des Untereozäns und einige Nummuliten des Ruchbergsandsteins. *Eclogae Geologicae Helvetiae, 28*, 641–648.
Baumfalk, Y. A., & Van Hinte, J. E. (1985). Orbitoides media (d'Archiac) in the Campanian deposits of the A 10 motorway at Mirambeau (Charente maritime). *Cretaceous Research, 6*(1–2), 181–189.
Beltrando, M., Frasca, G., Compagnoni, R., & Vitale-Brovarone, A. (2012). The Valaisan controversy revisited: Multi-stage folding of a Mesozoic hyper-extended margin in the Petit St. Bernard pass area (Western Alps). *Tectonophysics, 579*, 17–36. https://doi.org/10.1016/j.tecto.2012.02.010
Beltràn-Triviño, A., Winkler, W., & Von Quadt, A. (2013). Tracing Alpine sediment sources through laser-ablation U-Pb dating and Hf-isotopes of detrital zircons. *Sedimentology, 60*, 197–224.
Beltràn-Triviño, A., Winkler, W., Von Quadt, A., & Gallhofer, D. (2016). Triassic magmatism on the transition from Variscan to Alpine cycles: Evidence from U-Pb, Hf, and geochemistry of detrital minerals. *Swiss Journal of Geosciences, 109*, 309–328. https://doi.org/10.1007/s00015-016-0234-3
Bernoulli, D., & Weissert, H. (1985). Sedimentary fabrics in Alpine ophicalcites, South-Penninic Arosa zone, Switzerland. *Geology, 13*, 755–758.
Bertrand, A., & Sue, C. (2017). Reconciling late faulting over the whole Alpine belt: From structural analysis to geochronological constrains. *Swiss Journal of Geoscience, 110*, 565–580. https://doi.org/10.1007/s00015-017-0265-4
Blumental, M. M. (1931). Der Prättigauflysch und seine Stellung im Penninikum. *Eclogae Geologicae Helvetiae, 24*, 225–233.
Boudaugher-Fadel, M. K. (2018). *Evolution and geological significance of larger benthic foraminifera* (2nd ed., p. 702). UCL Press.
Bousquet, R., Goffé, B., Vidal, O., Oberhänsli, R., & Patriat, M. (2002). The tectono-metamorphic history of the Valaisan domain from the Western to the central Alps: New constraints on the evolution of the Alps. *Geological Society of America Bulletin, 114*, 207–225. https://doi.org/10.1130/0016-7606(2002)114%3c0207:TTMHOT%3e2.0.CO;2
Bundesamt Für Landestopografie *swisstopo* (2005). Geologische Karte der Schweiz 1:500'000. Wabern/Bern. https://s.geo.admin.ch/914563ea2f
Burla, St. (1997). Stratigraphie, Sedimentologie und Tektonik der nordpenninischen Serien in der Stätzerhornkette (Lenzerheide). Unpubl. Master Thesis ETH-Zürich, 109 pp.
Caron, C., Homewood, P., & Wildi, W. (1989). The original Swiss flysch: A reappraisal of the type deposits in the Swiss prealps. *Earth-Science Reviews, 26*(1–3), 1–45.
Ceccato, A., & Pennacchioni, G. (2018). Structural evolution of the Rieserferner pluton in the framework of the Oligo-Miocene tectonics of the Eastern Alps. *Journal of Structural Geology, 116*, 64–80.
De Broucker, G., Siméon, Y., Stampfli, G. M., Thiéblemont, D., Lach, Ph., & Marthaler, M. (2021). Early Cretaceous accretionary complex of the Valaisan Ocean, Western Alps? *Ofioliti, 46*(2), 203–227. https://doi.org/10.4454/ofioliti.v46i2.547
Ferreiro Mählmann, R., & Frey, M. (2012). Standardisation, calibration and correlation of the Kübler-index and the vitrinite/bituminite reflectance: An inter-laboratory and field related study. *Swiss Journal Geosci., 105*, 153–170. https://doi.org/10.1007/s00015-012-0110-8
Ferreiro Mählmann, R., Petrova, T., Pironon, J., Stern, W. B., Ghanbaja, J., Dubessy, J., & Frey, M. (2002). Transmission electron microscopy study of carbonaceous material in a metamorphic profile from diagenesis to amphibolite facies (Bündnerschiefer, Eastern Switzerland). *Schweizerische Mineralogische Und Petrographische Mitteilungen, 82*(2), 253–272.
Frey, M., Desmons, J., & Neubauer, F. (eds, 1999): The new metamorphic map of the Alps. Schweiz. Mineral. Petrogr. Mitt. 79/1, 236 p.
Frey, M., & Ferreiro Mählmann, R. (1999). Alpine metamorphism of the Central Alps. *Schweizerische Mineralogische Und Petrographische Mitteilungen, 79*, 135–154.
Furrer, H., Schaltegger, U., Ovtcharova, M., & Meister, P. (2008). U-Pb zircon age of volcaniclastic layers in Middle Triassic platform carbonates of the Austroalpine Silvretta nappe (Switzerland). *Swiss Journal of Geosciences, 101*, 595–603.
Gasinski, A., Slaczka, A., & Winkler, W. (1997). Tectono-sedimentary evolution of the Upper Prealpine nappe (Switzerland and France). nappe formation by Late Cretaceous-Paleogene accretion. *Geodinamica Acta, 10*, 137–157.
Gradstein, F. M., Ogg, J. G., Schmitz, M., & Ogg, G. (2013). *The geologic time scale 2012* (p. 176). Elsevier.
Guillong, M., von Quadt, A., Sakata, S., Peytcheva, I., & Bachmann, O. (2014). LA-ICP-MS Pb–U dating of young zircons from the Kos-Nisyros volcanic centre, SE Aegean arc. *Journal of Analytical Atomic Spectrometry, 29*, 963–970.
Häfner, W. (1924). Geologie des südöstlichen Rhätikon. Beitr. Geol. Karte der Schweiz, N.F. 54.1, 33 p.
Handy, K. R., Schmid, S. M., Bousquet, R., Kissling, E., & Bernoulli, D. (2010). Reconciling plate-tectonic reconstructions of Alpine Tethys with the geological–geophysical record of spreading and subduction in the Alps.

Earth-Science Reviews, 102, 121–158. https://doi.org/10.1016/j.earscirev.2010.06.002
Herwegh, M., Berger, A., Baumberger, R., Wehrens, Ph., & Kissling, E. (2017). Large-scale crustal-block-extrusion during late Alpine collision. *Scientific Reports, 7*(1), 413. https://doi.org/10.1038/s41598-017-00440-0
Jäckli, H. (1941). Geologische Untersuchungen im Westschams. *Eclogae Geologicae Helvetiae, 34*, 18–105.
Jackson, S. E., Pearson, N. J., Griffin, W. L., & Belousova, E. A. (2004). The application of laser ablation-inductively coupled plasma-mass spectrometry to in situ U-Pb zircon geochronology. *Chemical Geology, 211*, 47–69.
Kaneko, Y., Katayama, I., Yamamoto, H., Misawa, K., Ishikawa, M., Rehman, H. U., Kausar, A. B., & Shiraishi, K. (2003). Timing of Himalayan ultrahigh-pressure metamorphism: Sinking rate and subduction angle of the Indian continental crust beneath Asia. *Journal of Metamorphic Geology, 21*, 589–599.
Kästle, E. D., Rosenberg, C., Boschi, L., Bellahsen, N., Meier, Th., & El-Sharkawy, A. (2020). Slab break-offs in the Alpine subduction zone. *International Journal of Earth Sciences, 109*, 587–603.
Kotowski, A. J., Cisneros, M., Behr, W. M., Stockli, D. F., Soukis, K., Barnes, J. D., & Ortega-Arroyo, D. (2022). Subduction, underplating, and return flow recorded in the Cycladic Blueschist Unit exposed on Syros, Greece. *Tectonics, 41*, e2020TC006528. https://doi.org/10.1029/2020TC006528
Lihou, J. C., & Mange-Rajetzky, M. A. (1996). Provenance of the Sardona Flysch, eastern Swiss Alps: Example of high-resolution heavy mineral analysis applied to an ultrastable assemblage. *Sedimentary Geology, 105*, 141–157.
Loprieno, A., Bousquet, R., Bucher, S., Ceriani, S., Dalla Torre, F. H., Fügenschuh, B., & Schmid, S. M. (2011). The Valais units in Savoy (France): A key area for understanding the palaeogeography and the tectonic evolution of the Western Alps. *International Journal of Earth Sciences, 100*, 963–992.
Lu, G., Di Capua, A., Winkler, W., Rahn, M., Guillong, M., von Quadt, A., & Willett, S. D. (2019). Restoring the source-to-sink relationships in the Paleogene foreland basins in the Central and Southern Alps (Switzerland, Italy, France): A detrital zircon study approach. *International Journal of Earth Sciences, 108*, 1817–1834. https://doi.org/10.1007/s00531-019-01734-6
Lüdin, P. (1987) Flysch- und Melangebildungen in der südpenninischlunter-ostalpinen Arosa-Zone (Mittelbünden und Rätikon, Schweiz). PhD Thesis (unpubl.), Univ. Basel, 281 pp.
Manatschal, G., & Müntener, O. (2008). A type sequence across an ancient magma-poor ocean–continent transition: The example of the western Alpine Tethys ophiolites. *Tectonophysics*. https://doi.org/10.1016/j.tecto.2008.07.021
Matter, A., Homewood, P., Caron, C.; Rigassi, D., van Stuijvenberg, J., Weidmann, M. & Winkler, W. (1980). Flysch and Molasse of Western and Central Switzerland. In *Geology of Switzerland Exc. Guidebook No. 126A, Proceedings of the 26th International Geological Congress, Paris, France, 15 January 1980*; Geol. Komm.; Wepf & Co. Basel, Switzerland.
McCarthy, A., Chelle-Michou, C., Müntener, O., & Arculus Blundy, R. J. (2018). Subduction initiation without magmatism: The case of the missing Alpine magmatic arc. *Geology, 46*, 1059–1062. https://doi.org/10.1130/G45366.1
Moulas, E., Brandon, M. T., Hammon, J. T. V., Stefan, M., & Schmalholz, S. M. (2021). On backflow associated with oceanic and continental subduction. *Geophysical Journal International, 227*, 576–590.
Nänny, P. (1946). Neuere Untersuchungen in Prättigauflysch. *Eclogae Geologicae Helvetiae, 39*(2), 115–131.
Nänny, P. (1948). Zur Geologie der Prätigauschiefer zwischen Rhätikon und Plessur.- Mitteilungen aus dem Geologischen Institut der Eidgenössischen Technischen Hochschule und der Universität Zürich, 30, 127 pp.
Petrova, T. V., Ferreiro Mählmann, R., Stern, W. B., & Frey, M. (2002). Application of combustion and DTA-TGA analysis to the study of metamorphic organic matter. *Schweizerische Mineralogische Und Petrographische Mitteilungen, 82*, 33–53.
Petrus, J. A., & Kamber, B. S. (2012). Vizual Age: A novel approach to laser ablation ICP-MS U-Pb geochronology data reduction. *Geostandards and Geoanalytical Research, 36*, 247–270.
Pfiffner, A. (1992). Alpine Orogeny. In D. Blundell, R. Freeman, & S. Mueller (Eds.), *A Continent Revealed; The European Geotraverse* (pp. 187–197). Cambridge University Press.
Pfiffner, O. A. (2014). *Geology of the Alps* (2nd ed., p. 376). Oxford: John Wiley & Sons.
Pfiffner, O. A., Ellis, S., & Beaumont, C. (2000). Collision tectonics in the Swiss Alps Insight from geodynamic modeling. *Tectonics, 19*, 1065–1094.
Picazo, S. M., Ewing, T. A., & Müntener, O. (2019). Paleocene metamorphism along the Pennine-Austroalpine suture constrained by U-Pb dating of titanite and rutile (Malenco, Alps). *Swiss Journal of Geosciences, 112*, 517–542.
Price, J. B., Wernicke, B. P., Cosca, M. A., & Farley, K. A. (2018). Thermochronometry across the Austroalpine-Pennine boundary, Central Alps, Switzerland: Orogen-perpendicular normal fault slip on a major "overthrust" and its implications for orogenesis. *Tectonics, 37*, 724–757. https://doi.org/10.1002/2017TC004619
Ratschbacher, L., Frisch, W., Linzer, H.-G., & Merle, O. (1991). Lateral extrusion in the Eastern Alps, part 2: Structural analysis. *Tectonics, 10*, 257–271.
Rauch, A. (2014). Structural and stratigraphic relationships between ophiolite and sedimentary cover at Piz Mundin, Lower Engadine window, GR, CH. Unpubl. Master Thesis, Geneva University, 118 pp.
Ribes, C., Manatschal, G., Ghienne, J. F., Galster, F., Karner, G. D., Figueredo, P. H., Johnson, C. A., & Karpoff, A.-M. (2019). The syn-rift stratigraphic record across a fossil hyper-extended rifted margin: The example of the northwestern Adriatic margin exposed in the Central Alps. *Int J Earth Sci (geol Rundsch), 108*, 2071–2095. https://doi.org/10.1007/s00531-019-01750-6
Schaub, H. (1981). Nummulites et Assilines de la Téthys paléogène. Taxonomie, phylogenèse et biostratigraphie. Schweizerische paläontologisch Abhandlungen 104–106, 236 pp.
Schmid, S. M., Fügenschuh, B., Kissling, E., & Schuster, R. (2004). Tectonic Map and Overall Architecture of the Alpine Orogen. *Eclogae Geologicae Helvetiae, 97*, 93–117. https://doi.org/10.1007/s00015-004-1113-x
Schmid, S. M., Pfiffner, O. A., Froitzheim, N., Schönborn, G., & Kissling, E. (1996). Geophysical-geological transect and tectonic evolution of the Swiss-Italian Alps. *Tectonics, 15*, 1036–1064.
Schmid, S.M., Rück, PH., & Schreurs, G.: (1990). The significance of the Schams nappes for the reconstruction of the paleotectonic and orogenic evolution of the Pennine zone along the NFP 20 East traverse (Grisons, eastern Switzerland). In. Roure, F., Heitzmann, P. & Polino, R. (Eds.) Deep Structure of the Alps. Mém. Soc. Géol. France 156, 263–287.
Schmid, S. M., Scharf, A., Handy, M. R., & Rosenberg, C. L. (2013). The Tauern Window (Eastern Alps, Austria): A new tectonic map, with cross-sections and a tectonometamorphic synthesis. *Swiss Journal Geoscience, 2013*(106), 1–32. https://doi.org/10.1007/s00015-013-0123-y
Schreurs, G. (1993). Structural analysis of the Schams nappes and adjacent tectonic units implications for the orogenic evolution of the Penninic zone in eastern Switzerland. *Bull Soc Géol. France, 164*, 415–435.
Serra-Kiel, J., Hottinger, L., Caus, E., Drobne, K., Ferrandèz, C., Kumar Jauhri, A., Less, G., Pavlovec, R., Pignatti, J., Samso, J. M., Schaub, H., Sirel, E., Strougo, A., Tambarau, Y., Tosquella, J., & Zakrevskaya, E. (1998). *Bull. Soc. Géol. France, 169*(2), 281–299.
Signer, A., Maggetti, M., Winkler, W., Weissert, H.J., Keller, F. & Pfiffner, O.A. (2018). Blatt 1197 Davos. Geol. Atlas Schweiz 1:25000, Erläuterungen 156.
Stahel, A.H. (1926). Geologische Untersuchungen im nordöstlichen Rhàthikon (mit geologischer Karte). Unpubl. Dissertation Univ. Zürich.
Stampfli, G. M., Borel, G., Marchant, R., & Mosar, J. (2002). Western Alps geological constraints on western Tethyan reconstructions. *J. Virtual Explorer, 8*, 77–106.
Steck, A., Masson, H., & Martin Robyr, M. (2015). Tectonics of the Monte Rosa and surrounding nappes (Switzerland and Italy): Tertiary phases of subduction, thrusting and folding in the Pennine Alps. *Swiss Journal Geosci, 108*, 3–34. https://doi.org/10.1007/s00015-015-0188-x
Steinmann, M. (1994). Ein Beckenmodell für das Nordpenninikum der Ostschweiz. *Jb. Geol. b.-A Wien, 137*, 675–721.
Steinmann, M., & Stille, P. (1999). Geochemical evidence for the nature of the crust beneath the eastern North Penninic basin of the Mesozoic Tethys Ocean. *Geologische Rundschau, 87*, 633–643.
Tesauro, M., Hollenstein, Ch., Egli, R., Geiger, A., Kahle, H.-G., et al. (2005). Continuous GPS and broad-scale deformation across the Rhine Graben and the Alps. *Int J Earth Sci (geol Rundsch), 2005*(94), 525–537. https://doi.org/10.1007/s00531-004-0453-0
Thum, I., & Nabholz, W. (1972). Zur Sedimentologie und Metamorphose der penninischen Flysch- und Schieferabfolgen im Gebiet Prättigau-Lenzerheide-Oberhalbstein. Beitr. Geol. Karte Schweiz, N.F. 144, 55 pp.
Trümpy, D. (1916). Geologische Untersuchungen im westlichen Rhätikon. Beitr. Geol.Karte der Schweiz, N.F. 46.2, 22 p.
Trümpy, R. (1980). Part A: An outline of the Geology of Switzerland. *Geology of Switzerland A guide book* (p. 104). Wepf.

Vermeesch, P. (2018). IsoplotR: A free and open toolbox for geochronology. *Geoscience Frontiers, 9*, 1479–1493. https://doi.org/10.1016/j.gsf.2018.04.001

von Quadt, A., Gallhofer, D., Guillong, M., Peytcheva, I., Waelle, M., & Sakata, S. (2014). U/Pb dating of CA/non-CA treated zircons obtained by LA-ICP-MS and CA-TIMS techniques: Impact for their geological interpretation. *Journal of Analytical Atomic Spectrometry, 29*, 1618–1629.

Weh, M. (1998) Tektonische Entwicklung der penninischen Sediment-Decken in Graubünden (Prättigau bis Oberhalbstein). Diss. Univ. Basel (unpubl.). 230 pp.

Weh, M. & Froitzheim, N. (2001). Penninic cover nappes in the Prättigau half-window (Eastern Switzerland): Structure and tectonic evolution.—Eclogae geol. Helv. 94/2, 237–252.

Wiederkehr, M., Bousquet, R., Schmid, S. M., & Berger, A. (2008). From subduction to collision: Thermal overprint of HP/LT meta-sediments in the north-eastern Lepontine Dome (Swiss Alps) and consequences regarding the tectono-metamorphic evolution of the Alpine orogenic wedge. *Swiss Journal Geosci, 101*, 127–155.

Wiederkehr, M., Sudo, M., Bousquet, R., Berger, A., & Schmid, S. M. (2009). Alpine orogenic evolution from subduction to collisional thermal overprint: The 40Ar/39Ar age constraints from the Valaisan Ocean, central Alps. *Tectonics*. https://doi.org/10.1029/2009TC002496

Winkler, W. (1988). Mid- to early Late Cretaceous flysch and melange formations in the western part of the Eastern Alps. Palaeotectonic Implications. *Jb. Geo.l b.-A .in Wien, 131*, 341–389.

Winkler, W., & Wiederkehr, M. (2019). Cenozoic basin inversion in the North Penninic Valais domain of Eastern Switzerland (Prättigau). Abstract. 17th Swiss Geoscience Meeting, Fribourg 2019.

Wyss, R. & Wiederkehr, M. (2017). Blatt 1215 Thusis—Geol. Atlas Schweiz 1:25000, Erläuterungen, 154 pp.

Young, J.R., Wade, B.S., & Huber, B.T. (eds) (2017). pforams@mikrotax website. 21 Apr. 2017. URL: pforams@mikrotax

Publisher's Note